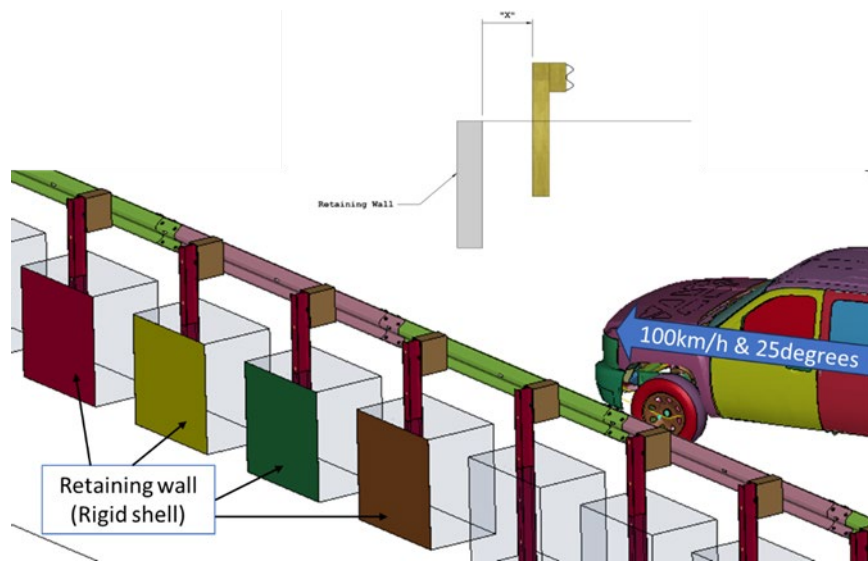


Project Report No. 619611



W-BEAM GUARDRAIL IN FRONT OF RETAINING WALL OR RIP RAP

Sponsored by
WASHINGTON STATE DEPARTMENT OF TRANSPORTATION (WSDOT)

TEXAS A&M TRANSPORTATION INSTITUTE
Roadside Safety & Physical Security
Texas A&M University System RELLIS Campus
Building 7091
1254 Avenue A
Bryan, TX 77807

1. Report No.		2. Government Accession No.		3. Recipient's Catalog No.	
4. Title and Subtitle W-beam Guardrail in Front of Retaining Wall or Rip Rap				5. Report Date August 2024	
				6. Performing Organization Code	
7. Author(s) Nauman M. Sheikh and Sun Hee Park				8. Performing Organization Report No. 619611	
9. Performing Organization Name and Address Texas A&M Transportation Institute 3135 TAMU College Station, Texas 77843-3135				10. Work Unit No. (TRAIS)	
				11. Contract or Grant No. Contract T1969-AC	
12. Sponsoring Agency Name and Address Washington State Department of Transportation Research Office MS 47372 Transportation Building Olympia, WA 98504-7372				13. Type of Report and Period Covered Technical Report: August 2024	
				14. Sponsoring Agency Code	
15. Supplementary Notes Name of Contacting Representative: Erik Emerson, P.E.					
16. Abstract <p>W-beam guardrail is often installed near a retaining wall or rip rap. Installing the guardrail too close to a retaining wall or rip rap can constrict the lateral movement of the guardrail posts that can degrade the ability of the guardrail to contain and redirect an impacting vehicle. Installation of the guardrail too close to a retaining wall can also result in additional loading on the wall due to the vehicle impact. This additional loading should be accounted for in the retaining wall design. Similarly, if the guardrail is installed too close to rip rap, an impacting vehicle can disturb the rip rap, resulting in costly repairs.</p> <p>This research provides additional loading on the retaining wall due to a vehicle impact on a guardrail that is installed adjacent to the retaining wall. Loading is provided for different lateral offsets of the W-beam guardrail from the retaining wall. This research also provides an optimal lateral offset between the W-beam guardrail and rip rap. This offset is expected to result in minimal disturbance of the rip rap due to a vehicle impact on the guardrail and allow the vehicle to redirect smoothly without riding over the rip rap.</p> <p>Findings of this research provide retaining wall design engineers with additional loading information to design safer retaining walls that can withstand the guardrail impact loading. It also provides minimum lateral offset guidance for guardrail installations adjacent to retaining walls and rip rap.</p>					
17. Key Words Retaining Wall, Rip Rap, W-beam, Guardrail, MGS, MASH, LS-DYNA, Simulation, Finite Element Model, FEA, Longitudinal Barrier, Design, Impact, Loads			18. Distribution Statement No restrictions. This document is available to the public through NTIS: National Technical Information Service Alexandria, Virginia 22312 http://www.ntis.gov		
19. Security Classification. (of this report) Unclassified		20. Security Classification. (of this page) Unclassified		21. No. of Pages 44	22. Price

Form DOT F 1700.7 (8-72) Reproduction of completed page authorized.

W-beam Guardrail in Front of Retaining Wall or Rip Rap

by

Nauman M. Sheikh, P.E.
Research Engineer
Texas A&M Transportation Institute

and

Sun Hee Park, Ph.D.
Associate Transportation Researcher
Texas A&M Transportation Institute

Report 619611
Contract No.: T1969-AC

Sponsored by the
Roadside Safety Research Pooled Fund

August 2024

TEXAS A&M TRANSPORTATION INSTITUTE
College Station, Texas 77843-3135

DISCLAIMER

The contents of this report reflect the views of the authors, who are solely responsible for the facts and accuracy of the data and the opinions, findings, and conclusions presented herein. The contents do not necessarily reflect the official views or policies of the Roadside Safety Research Pooled Fund, The Texas A&M University System, or the Texas A&M Transportation Institute (TTI). This report does not constitute a standard, specification, or regulation. In addition, the above listed agencies/companies assume no liability for its contents or use thereof. The names of specific products or manufacturers listed herein do not imply endorsement of those products or manufacturers.

The TTI's Roadside Safety and Physical Security Division strives for accuracy and completeness in its reports. On rare occasions, unintentional or inadvertent clerical errors, technical errors, omissions, oversights, or misunderstandings (collectively referred to as "errors") may occur and may not be identified for corrective action prior to the final report being published and issued. If, and when, TTI discovers an error in a published and issued final report, TTI will promptly disclose such error to the Roadside Safety Research Pooled Fund, and both parties shall endeavor in good faith to resolve this situation. TTI will be responsible for correcting the error that occurred in the report, which may be in the form of errata, amendment, replacement sections, or up to and including full reissuance of the report. The cost of correcting an error in the report shall be borne by TTI. Any such errors or inadvertent delays that occur in connection with the performance of the related testing contract will not constitute a breach of the testing contract.

TTI WILL NOT BE LIABLE FOR ANY INDIRECT, CONSEQUENTIAL, PUNITIVE, OR OTHER DAMAGES SUFFERED BY THE ROADSIDE SAFETY RESEARCH POOLED FUND OR ANY OTHER PERSON OR ENTITY, WHETHER SUCH LIABILITY IS BASED, OR CLAIMED TO BE BASED, UPON ANY NEGLIGENT ACT, OMISSION, ERROR, CORRECTION OF ERROR, DELAY, OR BREACH OF AN OBLIGATION BY TTI.

ACKNOWLEDGEMENTS

This research project was performed under a pooled fund program between the following States and Agencies. The authors acknowledge and appreciate their guidance and assistance.

Roadside Safety Research Pooled Fund Committee Revised April 2024

ALABAMA

Wade Henry, P.E.

Assistant State Design Engineer
Design Bureau, Final Design Division
Alabama Dept. of Transportation
1409 Coliseum Boulevard, T-205
Montgomery, AL 36110
(334) 242-6464
henryw@dot.state.al.us

Stanley (Stan) C. Biddick, P.E.

State Design Engineer
Alabama Dept. of Transportation
1409 Coliseum Boulevard, T-205
Montgomery, AL 36110
(334) 242-6488
biddicks@dot.state.al.us

ALASKA

Mary F. McRae

Assistant State Traffic & Safety Engineer
Alaska Depart. of Transportation & Public
Facilities
3132 Channel Drive
P.O. Box 112500
Juneau, AK 99811-2500
(907) 465-6963
mary.mcrae@alaska.gov

Micheal Hills

Alaska Depart. of Transportation & Public
Facilities
micheal.hills@alaska.gov

CALIFORNIA

Bob Meline, P.E.

Caltrans
Office of Materials and Infrastructure
Division of Research and Innovation
5900 Folsom Blvd
Sacramento, CA 95819
(916) 227-7031
Bob.Meline@dot.ca.gov

John Jewell, P.E.

Senior Crash Testing Engineer
Office of Safety Innovation & Cooperative
Research
(916) 227-5824
John.Jewell@dot.ca.gov

COLORADO

David Kosmiski, P.E.

Miscellaneous (M) Standards Engineer
Division of Project Support, Construction
Engineering Services (CES) Branch
Colorado Dept. of Transportation (CDOT)
2829 W. Howard Pl.
Denver, CO 80204
303-757-9021
david.kosmiski@state.co.us

Andy Pott, P.E.

Senior Bridge Design and Construction
Engineer
Division of Project Support, Staff Bridge
Design and Construction Management
Colorado Dept. of Transportation (CDOT)
4201 E Arkansas Ave, 4th Floor
Denver, CO 80222
303-512-4020
andrew.pott@state.co.us

Shawn Yu, P.E.

Miscellaneous (M) Standards and
Specifications Unit Manager
Division of Project Support, Construction
Engineering Services (CES) Branch
Colorado Dept. of Transportation (CDOT)
4201 E Arkansas Ave, 4th Floor
Denver, CO 80222
303-757-9474
shawn.yu@state.co.us

Amin Fakhimalizad

Assistant Miscellaneous (M) Standards
Engineer
Division of Project Support, Construction
Engineering Services (CES) Branch
Colorado Dept. of Transportation (CDOT)
303-757-9229
amin.fakhimalizad@state.co.us

Man (Steven) Yip

Division of Project Support, Construction
Engineering Services (CES) Branch
Colorado Dept. of Transportation (CDOT)
man.yip@state.co.us

CONNECTICUT**David Kilpatrick**

Transportation Supervising Engineer
State of Connecticut Depart. of
Transportation
2800 Berlin Turnpike
Newington, CT 06131-7546
(806) 594-3288
David.Kilpatrick@ct.gov

DELAWARE**Cassidy Blowers**

Construction Resource Engineer
Construction Section
Delaware DOT
(302)760-2336
Cassidy.Blowers@delaware.gov

James Osborne

Traffic Safety Programs Manager
Traffic Operations
Delaware DOT
(302)659-4651
James.Osborne@delaware.gov

FLORIDA**Richard Stepp**

Florida Department of Transportation
Richard.Stepp@dot.state.fl.us

Derwood C. Sheppard, Jr., P.E.

State Roadway Design Engineer
Florida Depart. of Transportation
Roadway Design Office
605 Suwannee Street, MS-32
Tallahassee, FL 32399-0450
(850) 414-4334
Derwood.Sheppard@dot.state.fl.us

IDAHO**Marc Danley, P.E.**

Technical Engineer
(208) 334-8558
Marc.danley@itd.idaho.gov

Kevin Sablan

Design/Traffic Engineer
Idaho Transportation Department
(208) 334-8558
Kevin.sablan@itd.idaho.gov

ILLINOIS**Martha A. Brown, P.E.**

Safety Design Bureau Chief
Bureau of Safety Programs and Engineering
Illinois Depart. of Transportation
2300 Dirksen Parkway, Room 005
Springfield, IL 62764
(217) 785-3034
Martha.A.Brown@illinois.gov

Edgar A. Galofre, MSCE, P.E.

Safety Design Engineer
Bureau of Safety Programs and Engineering
Illinois Department of Transportation
2300 S. Dirksen Parkway, Room 007
Springfield, IL 62764
(217) 558-9089
Edgar.Galofre@illinois.gov

IOWA**Daniel Harness**

Design Bureau – Methods Section
Iowa Department of Transportation
Daniel.Harness@iowadot.us

Chris Poole

State Traffic Engineer
Traffic and Safety Bureau
Iowa Department of Transportation
Chris.Poole@iowadot.us

LOUISIANA**Carl Gaudry**

Bridge Design Manager
Louisiana Department of Transportation and
Development
Bridge & Structural Design Section
P.O. Box 94245
Baton Rouge, LA 70804-9245
(225) 379-1075
Carl.Gaudry@la.gov

Chris Guidry

Assistant Bridge Design Administrator
Louisiana Department of Transportation and
Development
Bridge & Structural Design Section
P.O. Box 94245
Baton Rouge, LA 79084-9245
(225) 379-1328
Chris.Guidry@la.gov

MARYLAND**Philip Brentlinger**

Maryland State Highway Administration
pbrentlinger@mdot.maryland.gov

MASSACHUSETTS**James Danila**

Assistant State Traffic Engineer
Massachusetts Depart. of Transportation
(857) 368-9640
James.danila@state.ma.us

Alex Bardow

Director of Bridges and Structure
Massachusetts Depart. of Transportation
10 Park Plaza, Room 6430
Boston, MA 02116
(857) 368-9430
Alexander.Bardow@state.ma.us

MICHIGAN**Carlos Torres, P.E.**

Roadside Safety Engineer
Geometric Design Unit, Design Division
Michigan Depart. of Transportation
P. O. Box 30050
Lansing, MI 48909
(517) 335-2852
TorresC@michigan.gov

MINNESOTA**Khamsai Yang**

Design Standards Engineer
Office of Project Management and
Technical Support
(612) 322-5601
Khamsai.Yang@state.mn.us

Brian Tang

Assistant Design Standards Engineer
Office of Project Management and
Technical Support
Minnesota Department of Transportation
brian.tang@state.mn.us

MISSOURI**Amy Crawford**

Missouri Department of Transportation
105 West Capitol Avenue,
Jefferson City, Missouri 65102
Amy.Crawford@modot.mo.gov

Kaitlyn (Katy) Bower

Roadside Design Specialist
Missouri Department of Transportation
(573) 472-9028
kaitlyn.bower@modot.mo.gov

NEW MEXICO**Brad Julian**

New Mexico Department of Transportation
Traffic Technical Support Engineer
(505) 469-1405
Brad.Julian@dot.nm.gov

NEVADA

David Fox, P.E.

Specifications Engineer
Roadway Design Division
Nevada Dept. of Transportation
1263 S. Stewart St.
Carson City, NV 89712
(775) 888-7053
DWFox@dot.nv.gov

Tim Rudnick

Standards and Manuals Supervisor
Roadway Design Division
Nevada Dept. of Transportation
1263 S. Stewart St.
Carson City, NV 89712
(775) 888-7598
TRudnick@dot.nv.gov

OHIO

Don P. Fisher, P.E.

Ohio Depart. of Transportation
1980 West Broad Street
Mail Stop 1230
Columbus, OH 43223
(614) 387-2614
Don.fisher@dot.ohio.gov

OREGON

Christopher Henson

Senior Roadside Design Engineer
Oregon Depart. of Transportation
Technical Service Branch
4040 Fairview Industrial Drive, SE
Salem, OR 97302-1142
(503) 986-3561
Christopher.S.Henson@odot.state.or.us

PENNSYLVANIA

James A. Borino, Jr., P.E.

Chief, Standards and Criteria Unit
Highway Design and Technology Division
Pennsylvania DOT
(717) 612-4791
jborino@pa.gov

Evan Pursel

Senior Civil Engineer
Highway Design and Technology Division
Pennsylvania DOT

(717) 705-8535
epursel@pa.gov

Nina Ertel

Project Development Engineer
Highway Design and Technology Division
Pennsylvania DOT
(717) 425-7679
nertel@pa.gov

TENNESSEE

Laura Chandler

Engineering Production Support Manager
Engineering Division
Tennessee Dept. of Transportation
(615) 253-4769
Laura.Chandler@tn.gov

Ali Hangul M.S., P.E

State Standards Transportation Engineer
Engineering Production Support,
Engineering Division
Tennessee Dept. of Transportation
(615) 741-0840
Ali.Hangul@tn.gov

TEXAS

Chris Lindsey

Transportation Engineer
Design Division
Texas Department of Transportation
125 East 11th Street
Austin, TX 78701-2483
(512) 416-2750
Christopher.Lindsey@txdot.gov

Taya Retterer

TxDOT Bridge Standards Engineer
Bridge Division
Texas Department of Transportation
(512) 993-0330
Taya.Retterer@txdot.gov

Wade Odell

Research Project Manager
Research & Technology Implementation
Division
Texas Department of Transportation
(512) 416-4737
wade.odell@txdot.gov

UTAH**Matt Luker**

Utah Depart. of Transportation
4501 South 2700 West
PO Box 143200
Salt Lake City UT 84114-3200
(801) 440-9247
mluker@utah.gov

WASHINGTON**Tim Moeckel**

Roadside Safety Engineer
Washington State Department of
Transportation
Development Division
P.O. Box 47329
Olympia, WA 98504-7246
(360) 704-6377
moecket@wsdot.wa.gov

Mustafa Mohamedali

Research Manager/Engineering
Transportation Safety & System Analysis
Research & Library Services
(360) 704-6307
mohamem@wsdot.wa.gov

Kevin Burch

Policy Support Engineer
Washington State Department of
Transportation
Development Division
burchk@wsdot.wa.gov

WEST VIRGINIA**Donna J. Hardy, P.E.**

Mobility, ITS & Safety Engineer
West Virginia Depart. of
Transportation – Traffic Engineering
Building 5, Room A-550
1900 Kanawha Blvd E.
Charleston, WV 25305-0430
(304) 414-7338
Donna.J.Hardy@wv.gov

Ted Whitmore

Traffic Services Engineer
Traffic Engineering
WV Division of Highways
(304)414-7373
Ted.J.Whitmore@wv.gov

WISCONSIN**Erik Emerson, P.E.**

Standards Development Engineer –
Roadside Design
Wisconsin Department of Transportation
Bureau of Project Development
4802 Sheboygan Avenue, Room 651
P. O. Box 7916
Madison, WI 53707-7916
(608) 266-2842
Erik.Emerson@wi.gov

CANADA – ONTARIO**Kenneth Shannon, P. Eng.**

Senior Engineer, Highway Design (A)
Ontario Ministry of Transportation
301 St. Paul Street
St. Catharines, ON L2R 7R4
CANADA
(904) 704-3106
Kenneth.Shannon@ontario.ca

**FEDERAL HIGHWAY
ADMINISTRATION (FHWA)**

Website: safety.fhwa.dot.gov

Eduardo Arispe

Research Highway Safety Specialist
U.S. Department of Transportation
Federal Highway Administration
Turner-Fairbank Highway Research Center
Mail Code: HRDS-10
6300 Georgetown Pike
McLean, VA 22101
(202) 493-3291
Eduardo.arispe@dot.gov

Richard B. (Dick) Albin, P.E.

Senior Safety Engineer
Office of Innovation Implementation, Safety
& Design Team
(303) 550-8804
Dick.Albin@dot.gov

Matt Hinshaw, M.S., P.E.

Highway Safety Engineer
Central Federal Lands Highway Division
(360) 619-7677
matthew.hinshaw@dot.gov

Paul LaFleur, P.E.

Safety Design Team - Roadway Departure
Program Manager
FHWA Office of Safety
U.S. Department of Transportation
(515) 233-7308
paul.lafleur@dot.gov

Christine Black

Highway Safety Engineer
Central Federal Lands Highway Division
12300 West Dakota Ave.
Lakewood, CO 80228
(720) 963-3662
Christine.black@dot.gov

Isbel Ramos-Reyes

Lead Safety and Transportation Operations
Engineer
Eastern Federal Lands Highway Division

(703) 948-1442

isbel.ramos-reyes@dot.gov

**TEXAS A&M TRANSPORTATION
INSTITUTE (TTI)**

Website: tti.tamu.edu
www.roadsidepooledfund.org

D. Lance Bullard, Jr., P.E.

Senior Research Engineer
Roadside Safety & Physical Security Div.
Texas A&M Transportation Institute
3135 TAMU
College Station, TX 77843-3135
(979) 317-2855
L-Bullard@tti.tamu.edu

Roger P. Bligh, Ph.D., P.E.

Senior Research Engineer
Roadside Safety and Physical Security
Division
(979) 317-2703
R-Bligh@tti.tamu.edu

Nauman M. Sheikh, P.E.

Research Engineer
Roadside Safety and Physical Security
Texas A&M Transportation Institute
(979) 317-2703
n-sheikh@tti.tamu.edu

Ariel Sheil

Research Assistant
Roadside Safety and Physical Security
Texas A&M Transportation Institute
(979) 317-2250
A-Sheil@tti.tamu.edu

This page intentionally left blank.

TABLE OF CONTENTS

ACKNOWLEDGEMENTS	VIII
LIST OF FIGURES	VIII
LIST OF TABLES	IX
CHAPTER 1. INTRODUCTION	1
1.1. Background.....	1
1.2. Objectives	2
CHAPTER 2. RIP RAP OFFSET	3
CHAPTER 3. GUARDRAIL LOADING ON RETAINING WALL	5
3.1. Finite Element Model	5
3.2. Model Validation	7
3.3. Retaining Wall Load Distribution	14
3.3.1. Model Setup.....	14
3.3.2. Simulation Results	17
3.3.3. Implementation	23
CHAPTER 4. SUMMARY AND CONCLUSIONS	25
REFERENCES	26
APPENDIX A	27

LIST OF FIGURES

	Page
Figure 1.1. Example of Retaining Wall and Rip Rap Installed Adjacent to Guardrail.	2
Figure 2.1. Test 3-11 of W-beam Guardrail System with Pickup Truck [3].	3
Figure 3.1. Images of the Guardrail System Model and Key Components.....	6
Figure 3.2. Comparison of Vehicle Impact and Redirection.	8
Figure 3.3. RSVVP– Multi-Channel Validation Metrics.....	10
Figure 3.4. RSVVP– Y Acceleration (Lateral) Validation Metrics.	11
Figure 3.5. RSVVP– Yaw Angle Validation Metrics.....	12
Figure 3.6. RSVVP– X Acceleration (Longitudinal) Validation Metrics.	13
Figure 3.7. Soil Bucket Model and Dimensions.	14
Figure 3.8. Isometric View of the System Model and Locations of Load-Recording Regions on the Retaining Wall.	16
Figure 3.9. Location of Impact Point and Post with Largest Lateral Load.....	17
Figure 3.10. Sequential Images During Impact Simulations.....	18
Figure 3.11. Sequential Images During Impact Simulations.....	19
Figure 3.12. Pressure Loads on Retaining Wall for Different Offsets of the W-beam Guardrail.	20
Figure 3.13. Pressure Distribution on Retaining Wall with 3-ft Offset.....	21
Figure 3.14. Pressure on Retaining Wall as a Function of Depth.....	22
Figure 3.15. Pressure Loading on a Retaining Wall due to Impact on a W-beam Guardrail at 7-inch Offset.	23

LIST OF TABLES

	Page
Table 3.1. MASH Test 3-11 Occupant Risk Comparison.	8

SI* (MODERN METRIC) CONVERSION FACTORS

APPROXIMATE CONVERSIONS TO SI UNITS

Symbol	When You Know	Multiply By	To Find	Symbol
LENGTH				
in	inches	25.4	millimeters	mm
ft	feet	0.305	meters	m
yd	yards	0.914	meters	m
mi	miles	1.61	kilometers	km
AREA				
in ²	square inches	645.2	square millimeters	mm ²
ft ²	square feet	0.093	square meters	m ²
yd ²	square yards	0.836	square meters	m ²
ac	acres	0.405	hectares	ha
mi ²	square miles	2.59	square kilometers	km ²
VOLUME				
fl oz	fluid ounces	29.57	milliliters	mL
gal	gallons	3.785	liters	L
ft ³	cubic feet	0.028	cubic meters	m ³
yd ³	cubic yards	0.765	cubic meters	m ³
NOTE: volumes greater than 1000L shall be shown in m ³				
MASS				
oz	ounces	28.35	grams	g
lb	pounds	0.454	kilograms	kg
T	short tons (2000 lb)	0.907	megagrams (or metric ton")	Mg (or "t")
TEMPERATURE (exact degrees)				
°F	Fahrenheit	5(F-32)/9 or (F-32)/1.8	Celsius	°C
FORCE and PRESSURE or STRESS				
lbf	poundforce	4.45	newtons	N
lbf/in ²	poundforce per square inch	6.89	kilopascals	kPa

APPROXIMATE CONVERSIONS FROM SI UNITS

Symbol	When You Know	Multiply By	To Find	Symbol
LENGTH				
mm	millimeters	0.039	inches	in
m	meters	3.28	feet	ft
m	meters	1.09	yards	yd
km	kilometers	0.621	miles	mi
AREA				
mm ²	square millimeters	0.0016	square inches	in ²
m ²	square meters	10.764	square feet	ft ²
m ²	square meters	1.195	square yards	yd ²
ha	hectares	2.47	acres	ac
km ²	Square kilometers	0.386	square miles	mi ²
VOLUME				
mL	milliliters	0.034	fluid ounces	oz
L	liters	0.264	gallons	gal
m ³	cubic meters	35.314	cubic feet	ft ³
m ³	cubic meters	1.307	cubic yards	yd ³
MASS				
g	grams	0.035	ounces	oz
kg	kilograms	2.202	pounds	lb
Mg (or "t")	megagrams (or "metric ton")	1.103	short tons (2000lb)	T
TEMPERATURE (exact degrees)				
°C	Celsius	1.8C+32	Fahrenheit	°F
FORCE and PRESSURE or STRESS				
N	newtons	0.225	poundforce	lbf
kPa	kilopascals	0.145	poundforce per square inch	lb/in ²

*SI is the symbol for the International System of Units

Chapter 1. INTRODUCTION

1.1. BACKGROUND

There are many situations where W-beam guardrail is installed near retaining walls and rip rap (Figure 1.1). Installing the guardrail too close to a retaining wall or rip rap can restrict the lateral movement and rotation of the guardrail posts, which can adversely affect the guardrail's impact performance, or result in costly damage to the retaining wall or rip rap.

Guardrail posts require some soil around them to allow deflection and deformation of the posts during vehicular impact and redirection. If the deflection of the posts is constrained by placing them close to a concrete wall or by installing them in a constraining medium such as a concrete footing, thick asphalt, rock, etc., the posts bend prematurely at the ground level during a vehicle impact, which results in the guardrail system is not being able to contain and redirect the vehicle. Appendix A lists some of the research that has been performed to address movement of the posts for successful W-beam guardrail performance.

When the guardrail is installed near a retaining wall or rip rap, there is a need to determine the proper offset of the guardrail that maintains the MASH compliant performance of the guardrail and avoids damage to the retaining wall or rip rap. Furthermore, in situations when the guardrail is installed close to a retaining wall, additional loading on the wall due to vehicle impact with the guardrail needs to be determined so it can be incorporated in the design of the retaining wall.

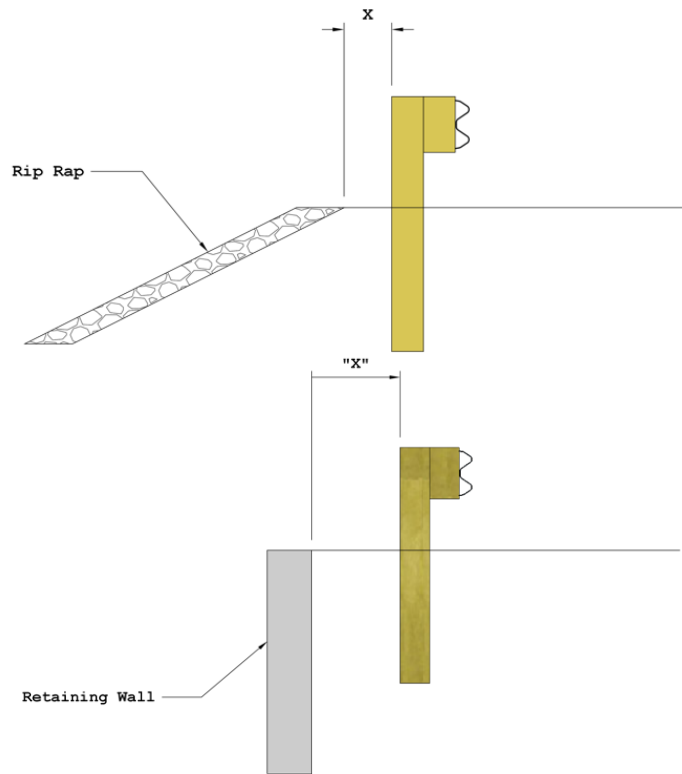


Figure 1.1. Example of Retaining Wall and Rip Rap Installed Adjacent to Guardrail.

1.2. OBJECTIVES

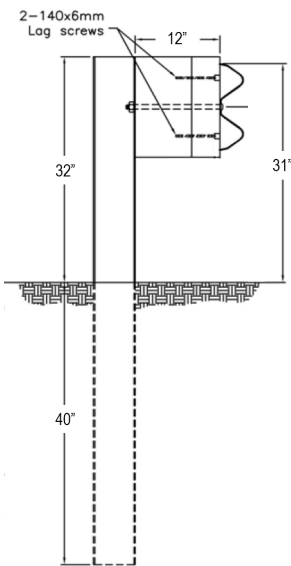
The objectives of this research were as follows:

1. Determine the minimum lateral offset distance between the W-beam guardrail and rip rap that causes minimal disturbance to rip rap.
2. Determine vehicle impact load transferred to the retaining wall by a W-beam guardrail installed adjacent to a retaining wall. This loading was to be provided for various lateral offsets of the W-beam guardrail from the retaining wall.
3. Provide guidance on the minimal lateral distance from the retaining wall that would allow proper functioning of the guardrail system in accordance with MASH Test Level 3 (TL-3) impact performance criteria.

Chapter 2. RIP RAP OFFSET

If rip rap is installed too close to a W-beam guardrail, the instability of an impacting vehicle that causes the guardrail to deflect laterally can increase if it rides over the rip rap. Presence of rip rap too close to the guardrail posts can also hinder proper lateral deflection and rotation of the posts, potentially resulting in deteriorated crash performance of the guardrail. Furthermore, displaced or dispersed rip rap results in additional maintenance cost when a guardrail system is repaired after vehicle impact. For these reasons, the research team suggests using a lateral offset that is approximately equivalent to the maximum dynamic deflection of the W-beam guardrail system. Using this offset is expected to result in minimal to no interaction between the impacting vehicle and rip rap.

Polivka et al. [3] evaluated the W-beam Midwest Guardrail System (MGS) in accordance with the Update to National Cooperative Highway Research Program (NCHRP) Report 350 evaluation criteria for Test 3-11. The vehicle impact conditions and evaluation criteria for Test 3-11 of the Update to NCHRP Report 350 were the same as MASH, i.e., a 5,000-lb pickup truck impacting the W-beam guardrail at an impact speed and angle of 62 mph and 25 degrees, respectively. Figure 2.1 shows the cross-section of the W-beam guardrail design, the test installation prior to test, and the deflection of the guardrail after the test. In this test, the maximum lateral dynamic deflection of the guardrail was 43.9 inches.



(a) Guardrail Cross-section



(b) Installation Before Test



(c) Installation After Test

Figure 2.1. Test 3-11 of W-beam Guardrail System with Pickup Truck [3].

To ensure that rip rap is minimally disturbed while a guardrail redirects a vehicle, it is therefore recommended that an offset of 44 inches, measured from the back of the guardrail posts, be used when installing the W-beam guardrail adjacent to rip rap. This offset also ensures the vehicle will not be traversing over rip rap, which can deteriorate the stability of the vehicle as previously mentioned.

Chapter 3. GUARDRAIL LOADING ON RETAINING WALL

To develop guidance for the lateral load applied on a retaining wall due to vehicle impact on a W-beam guardrail system that is installed at some offset from the wall, the researchers determined the loads using full-scale finite element (FE) simulations. The researchers developed a model of the W-beam guardrail system and validated the model using the results of the past Test 3-11 performed on the guardrail by Polivka et al. [3]. Once this model was validated, the researchers modeled a rigidized retaining wall to determine lateral loading applied to the wall when the vehicle impacted the guardrail. FE impact simulations were performed with the guardrail installed at varying offsets from the wall, enabling the researchers to obtain loads for different offsets of the guardrail from the retaining wall.

It should be noted that the loading determined in this research does not incorporate currently used loads or analysis methods for designing retaining walls. It is an additional loading that is applied to a retaining wall due to the vehicle impact on an adjacent W-beam guardrail.

All simulations were performed using LS-DYNA, which is a commercially available general-purpose FE analysis software [4]. Details of the FE model, its validation, analysis details for different guardrail offsets, and the recommended load guidelines for retaining wall design are presented in this chapter.

3.1. FINITE ELEMENT MODEL

The FE model of the W-beam guardrail was based on the test installation used by Polivka et al. in Test 2214MG-2 performed at MwRSF [3]. This guardrail system was comprised of the standard 12-gauge W-beam guardrail supported by W6X9 steel posts. The posts were spaced 75 inches in the center with a soil embedment depth of 40 inches. The W-beam rail was spaced away from the front face of the steel posts using 6 inches wide x 12 inches deep x 14.25 inches long wood blockouts. The height of the top of the W-beam rail was 31 inches. The rail splices were located midspan between adjacent posts. Further details of the system can be found in the MwRSF report.

Full-scale vehicle crash test using a pickup truck vehicle was performed on the guardrail system and was determined to be acceptable according to the Test 3-11 performance evaluation criteria presented in the Update to NCHRP Report No. 350, which is equivalent to MASH Test 3-11 evaluation criteria. This involved testing with a 5,000-lb pickup truck, impacting the guardrail at a speed of 62.5 mi/h, and at an angle of 25 degrees. The actual impact speed and impact angle in the test were 62.8 mi/h and 25.5 degrees, respectively, which were within the allowed tolerances.

In this test, the W-beam guardrail system had a maximum lateral permanent deflection of 31.6 inches. The maximum lateral dynamic deflection was 43.9 inches. Further details of the crash test results can be found in the test report.

Figure 3.1 presents images of the overall guardrail system model, as well as closer details of the various key components of the model. The overall system model was approximately 125 ft long and was comprised of 20 posts with 75-inch post

spacing. The key guardrail parts including the W-beam, posts, splices, and blockouts, were represented with elastic-plastic material models.

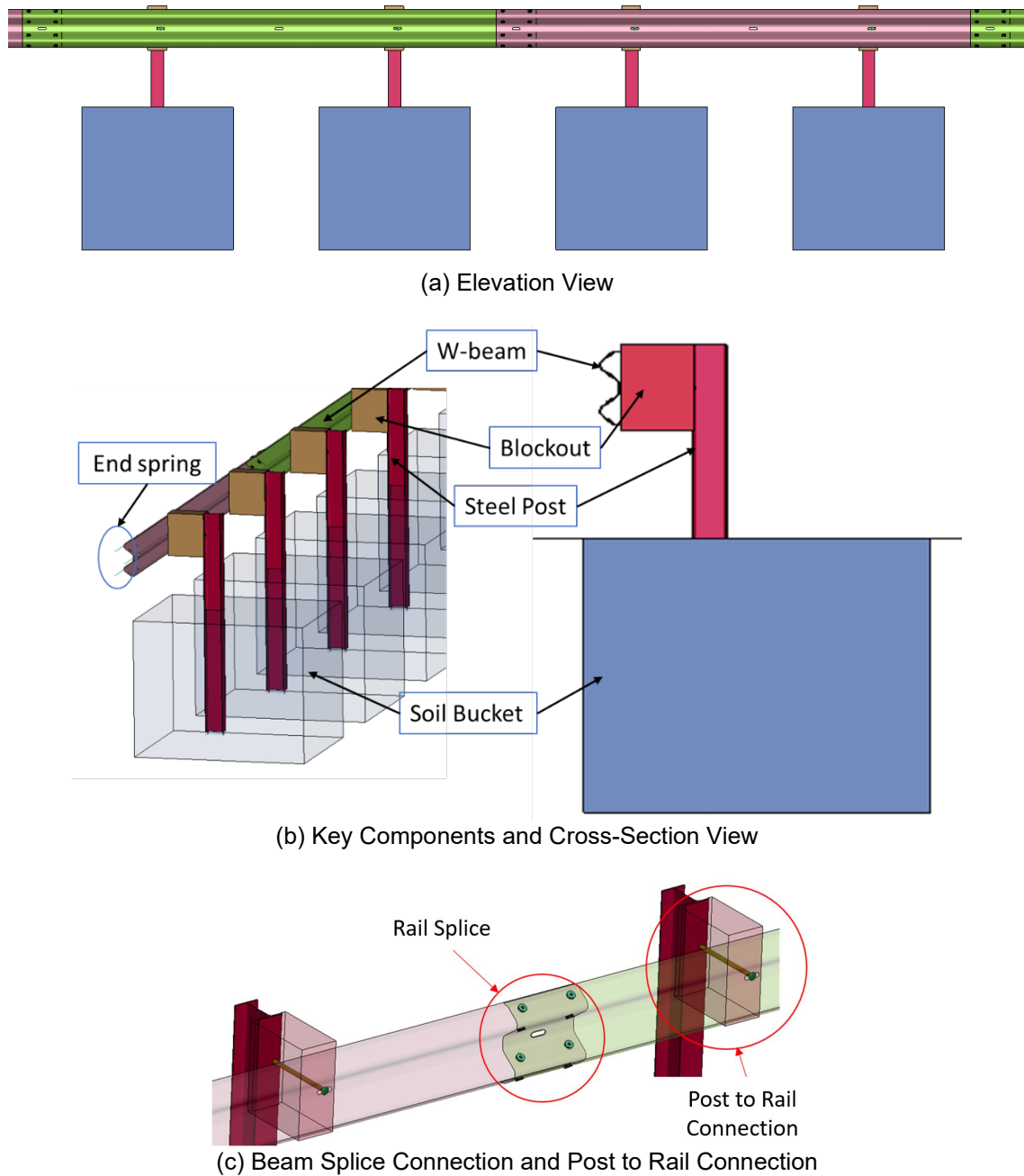


Figure 3.1. Images of the Guardrail System Model and Key Components.

W-beam rail segments and posts were meshed with shell elements. Since the W-beam works by maintaining tension in the rail element during impact, it was constrained at each end using spring elements. The force-deflection properties of these spring

elements have been previously calibrated by TTI researchers to represent the presence of a guardrail end terminal.

Wood blockouts and posts were meshed with solid elements. The W-beam rail and the wood blockouts were bolted to the flange of the posts with a bolt model that was comprised of beam and shell elements.

The posts were placed inside soil buckets which were meshed with solid elements. The soil buckets were modeled with deformable material representing soil properties. The posts were modeled unconstrained and were free to deflect and rotate in the soil continuum due to the impact loading. The boundaries of the soil buckets were constrained to maintain the shape of the soil bucket and to prevent them from falling under gravity load.

While MASH Test Level 3 (TL-3) requires testing the guardrail system with a small passenger sedan in addition to the pickup truck, the small car is not expected to impart greater load into an adjacent retaining wall compared to the heavier pickup truck. For this reason, impact simulations were only performed using the pickup truck under MASH Test 3-11 conditions. This provided loading information for the more critical of the two test conditions required by MASH TL-3.

A publicly available model of a 2007 Chevrolet Silverado [5], which was developed by the National Crash Analysis Center and Center for Collision Safety and Analysis, was used in the simulation analyses. This model has been further improved by the research team over the course of various research projects to achieve greater validation and robustness.

3.2. MODEL VALIDATION

To check the validity of the FE model, results of an impact simulation with the W-beam guardrail model were compared to the MwRSF Test 2214MG-2. To replicate the impact conditions of Test 2214MG-2, the vehicle model was set with an initial speed and angle of 62.8 mi/h and 25.5 degrees, respectively. Figure 3.2 compares sequential frames from full-scale Test 2214MG-2 and the corresponding FE simulation. The containment and redirection behavior of the vehicle at each time frame shows a similar trend in the simulation when compared to the test results.

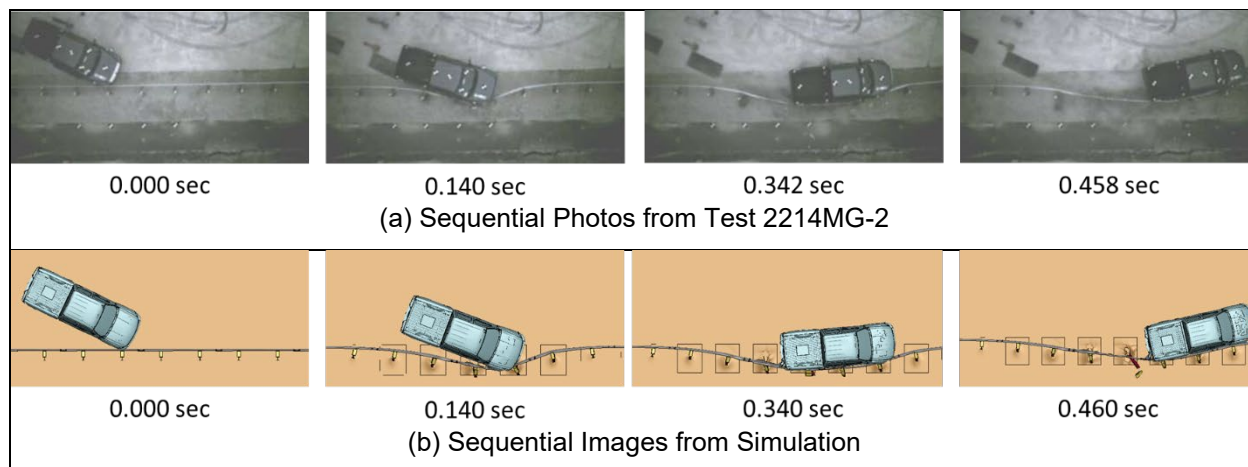


Figure 3.2. Comparison of Vehicle Impact and Redirection.

Test Risk Assessment Program (TRAP) [6] was used to evaluate the occupant risk factors based on the applicable MASH [2] safety evaluation criteria. Table 3.1 compares the key occupant risk parameters from MwRSF Test 2214MG-2 and the impact simulation performed to validate the FE model. The values from the simulation were reasonably validated with the test values.

Table 3.1. MASH Test 3-11 Occupant Risk Comparison.

		Test 2214MG-2	FE Model
Impact Velocity (ft/s)	Longitudinal	15.32	16.9
	Lateral	15.62	14.8
Ride down Acceleration (g)	Longitudinal	8.23	11.4
	Lateral	6.93	10.0
Maximum Deflection (in.)	Permanent	31.6	36.2
	Dynamic	43.9	49.3

Roadside Safety Verification and Validation Program (RSVVP) was used to compare the similarity of time-history signals from the test and the simulation data by computing the Sprague-Geer metrics and ANOVA metrics [7,8]. The six data signals analyzed for validation were the x-acceleration (longitudinal), y-acceleration (lateral), z-acceleration (vertical), roll-rate, pitch-rate, and yaw-rate of the vehicle near its center of gravity. Using the RSVVP software, each of the individual data types were analyzed and compared between the simulation and test results. Furthermore, a multi-channel comparison was made for all six data time-histories using the weighted composite of the six data signals. The analysis of all validation metrics was performed using the guidelines and thresholds established by the verification and validation guidelines provided in NCHRP Document 179 [8].

To analyze validation of the data between test and simulation, the research team used two different time intervals. These were from 0.0 to 0.3 seconds and from 0.0 to 0.7 seconds. The 0.0 to 0.3-second interval was selected to check the model's validity in the earlier part of the impact and redirection, when maximum lateral load is applied to the W-beam guardrail system and any retaining wall that may be placed in later

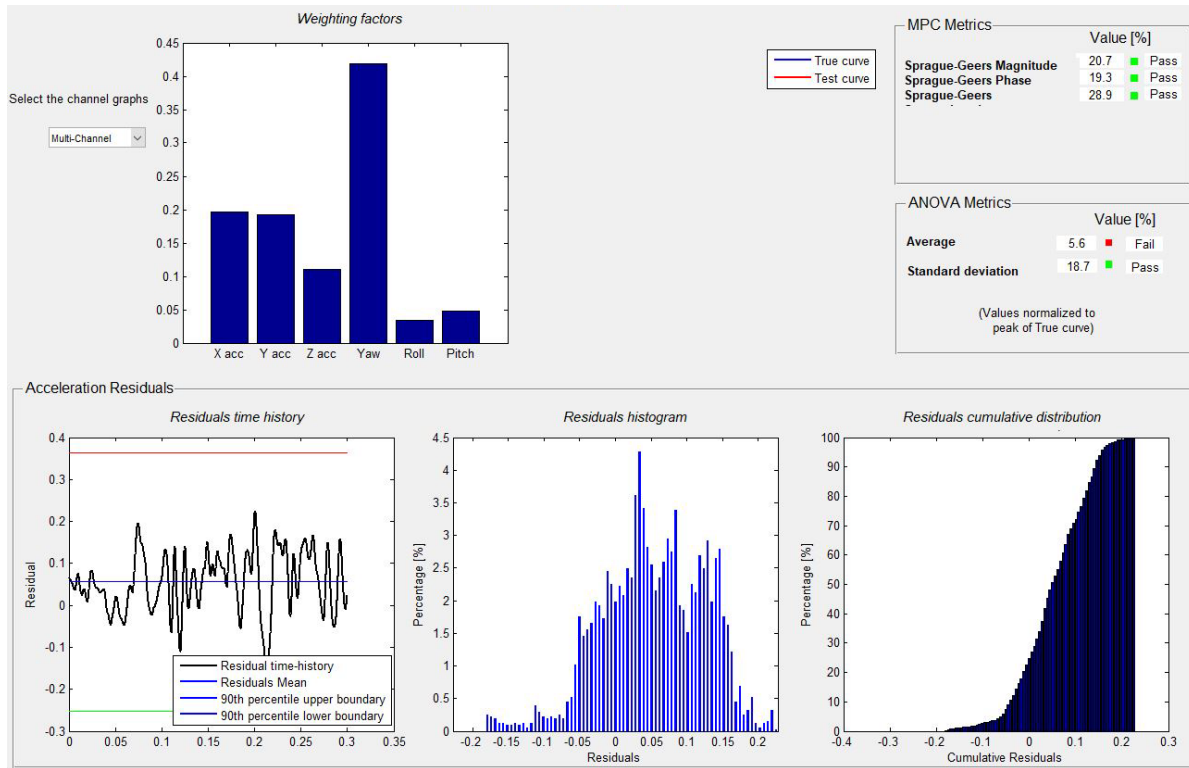
simulations. The 0.0 to 0.7-second interval was selected since it was the approximate duration of the entire impact and redirection event, thus enabling the validation evaluation for the overall test and simulation interval.

Figure 3.3 through Figure 3.6 show the results of the validation analysis using RSVVP for both time intervals. Figure 3.3 shows the multi-channel weighted validation analysis which uses all six data signals measured in the test. For the 0.0 to 0.3-second interval, the results were within the acceptable validation thresholds established by NCHRP Document 179 except for ANOVA Average, which was slightly above the threshold (5.6% instead of the $\leq 5\%$ threshold). For the 0.0 to 0.7-second interval, all five metrics were within the thresholds established by NCHRP Document 179. These results showed good overall validation of the W-beam guardrail model compared to the test results.

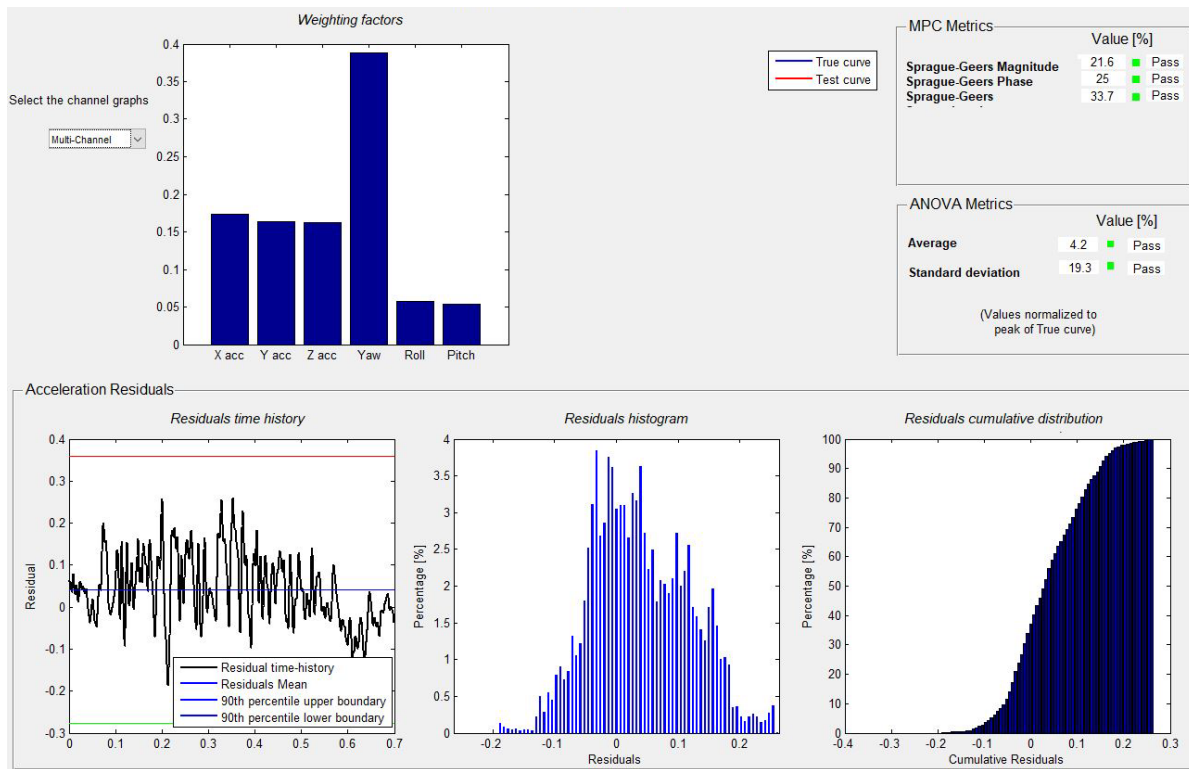
The multi-channel validation analysis results between 0.0 to 0.3-second time interval in Figure 3.3 also show that the x-acceleration, y-acceleration, and yaw rate were the most significant data signals for the initial impact and redirection phase when the maximum load is applied to the guardrail. From the perspective of lateral load transfer on the guardrail, the y-acceleration and the yaw rate are the most significant metrics that represent the lateral deceleration and redirection of the vehicle.

Figure 3.4 shows the validation analysis of the y-acceleration for both time intervals. The simulation results passed all five validation metrics established by NCHRP Document 179. Figure 3.5 shows the validation analysis of the yaw rate for both time intervals. In this case also, the simulation results passed all validation metrics established by NCHRP Document 179.

Figure 3.6 shows the validation analysis of the x-acceleration for both time intervals. In this case, the simulation model passed all but one metric, which was ANOVA Average. While this metric was exceeded in the model, the fact that the remaining four metrics were within the validation thresholds and that for transfer of lateral load on the guardrail, x-acceleration is less critical compared to y-acceleration and yaw rate, the researchers determined that the model was sufficiently valid for further use in the project.

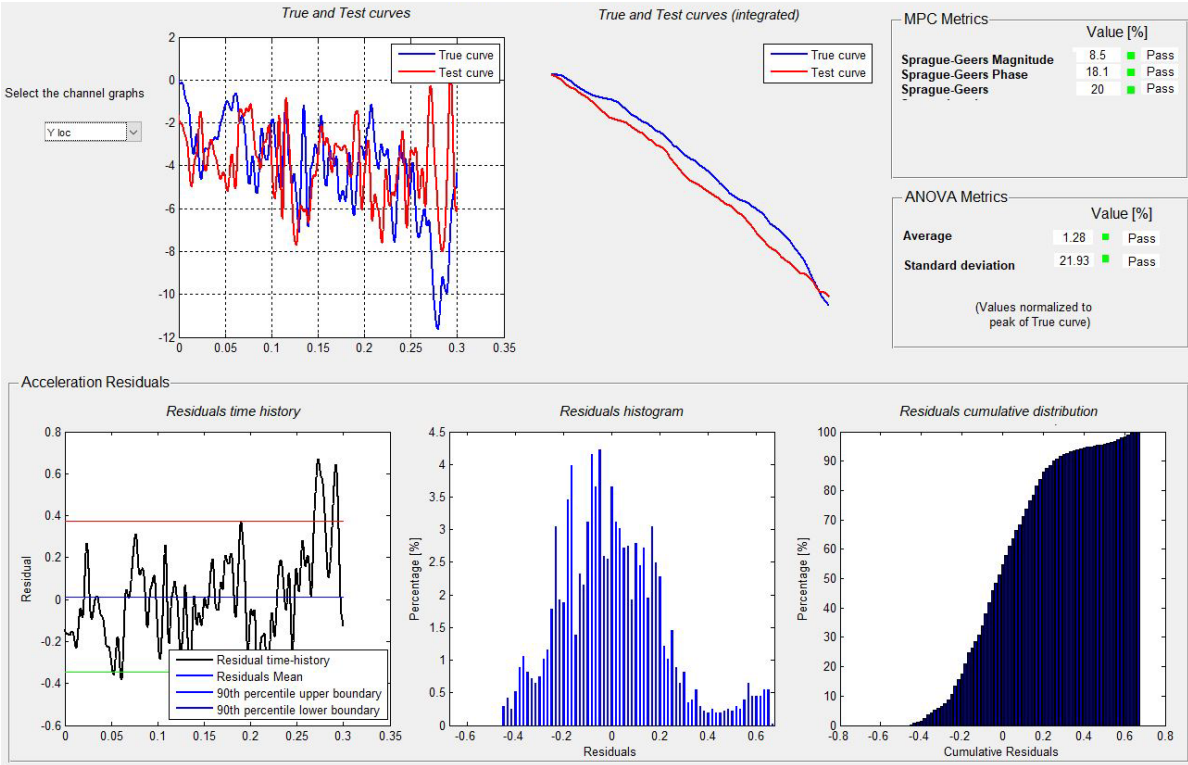


(a) 0.0 sec – 0.3 sec

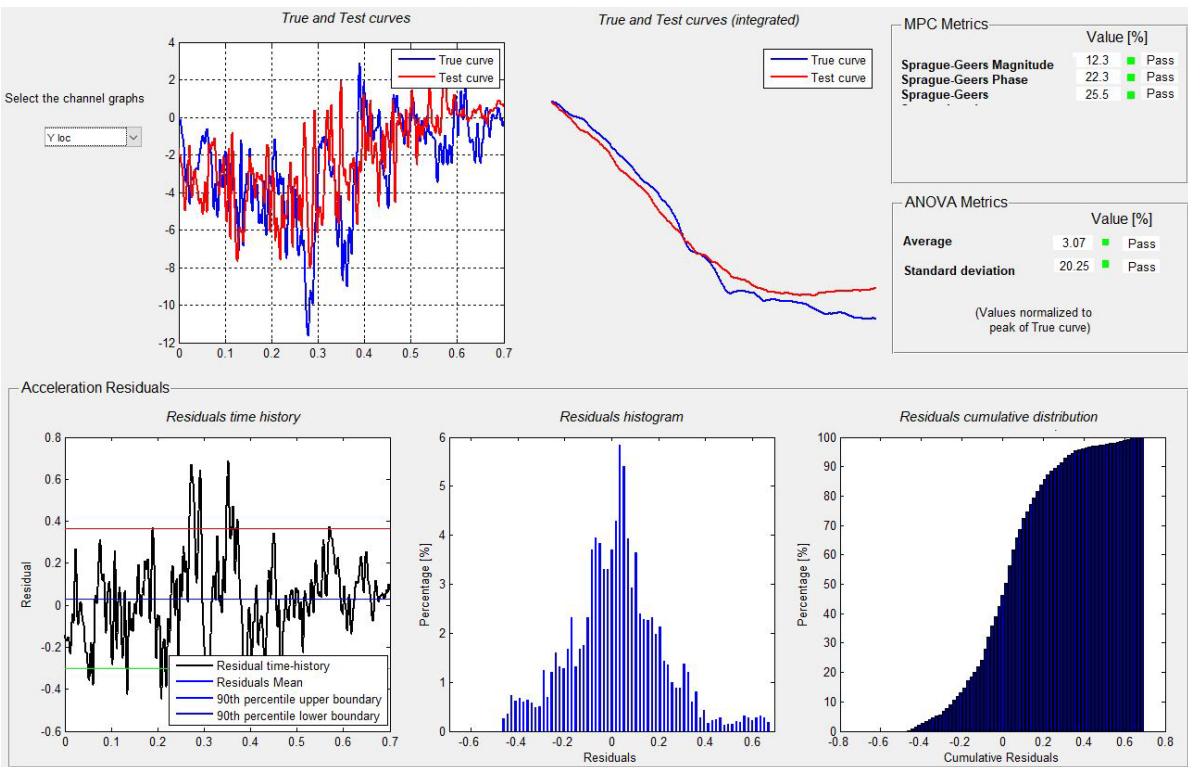


(b) 0.0 sec – 0.7 sec

Figure 3.3. RSVVP– Multi-Channel Validation Metrics.

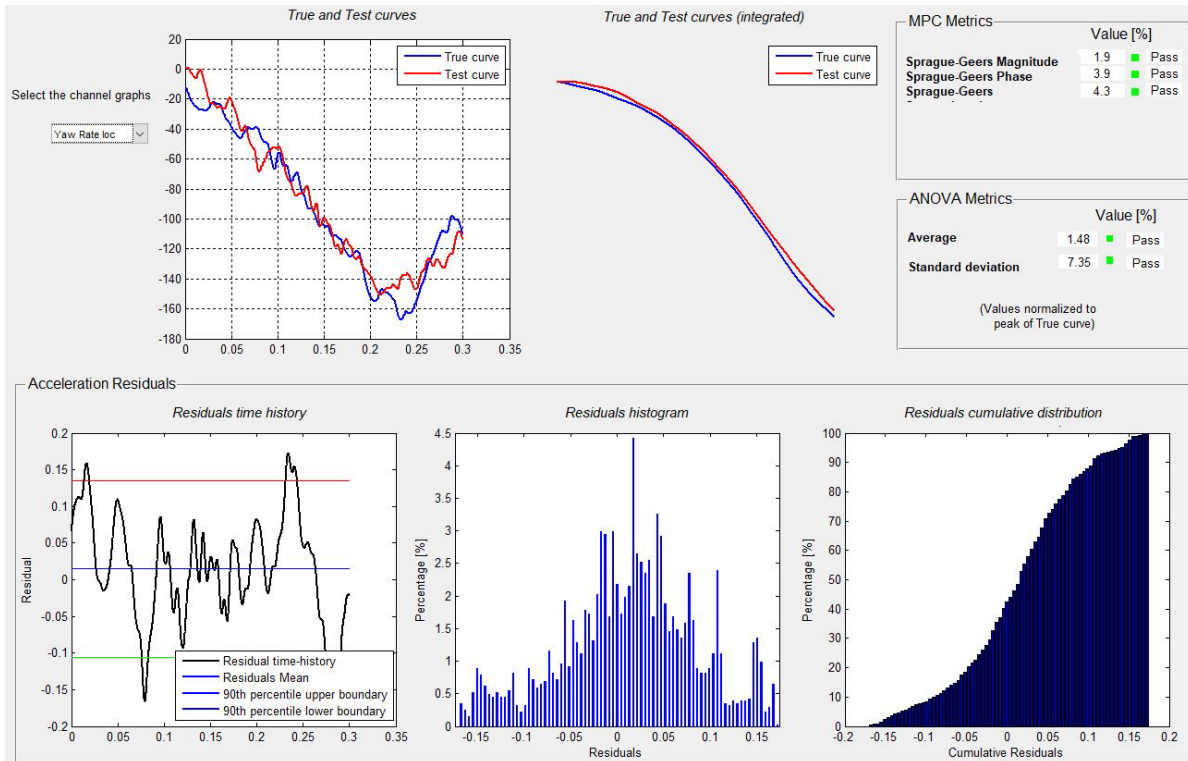


(a) 0.0 sec – 0.3 sec

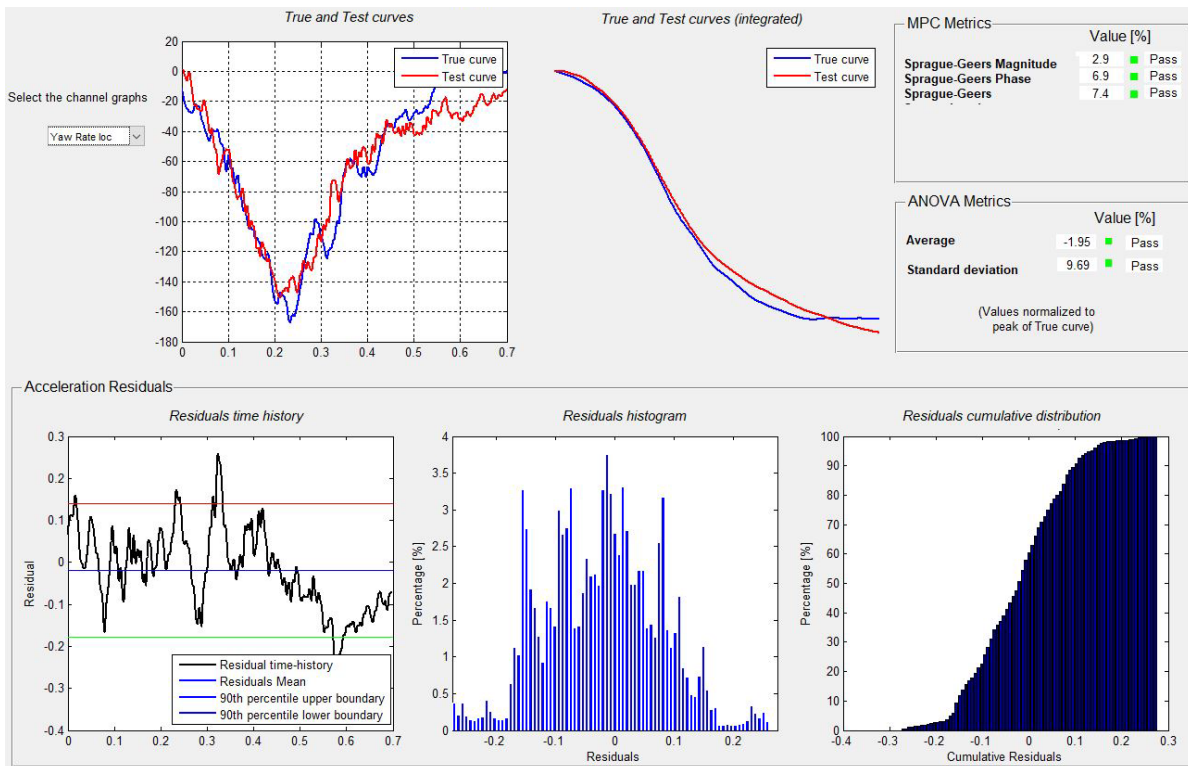


(b) 0.0 sec – 0.7 sec

Figure 3.4. RSVVP– Y Acceleration (Lateral) Validation Metrics.

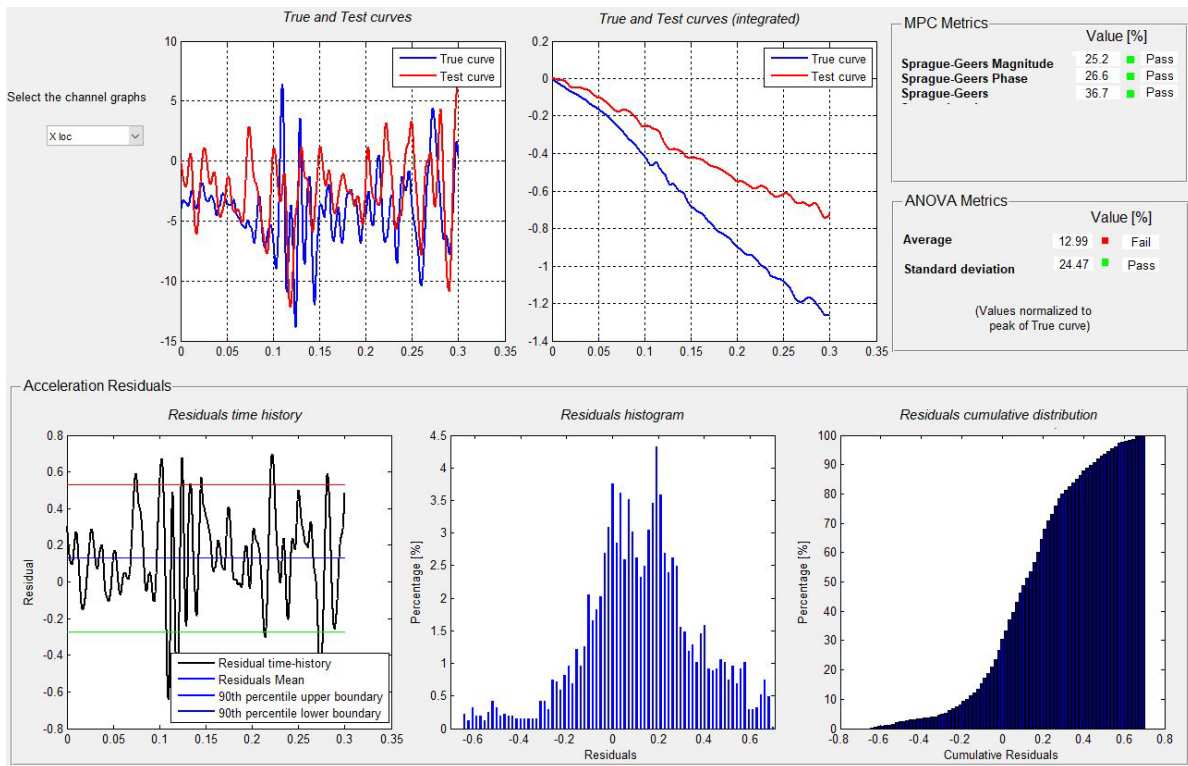


(a) 0.0 sec – 0.3 sec

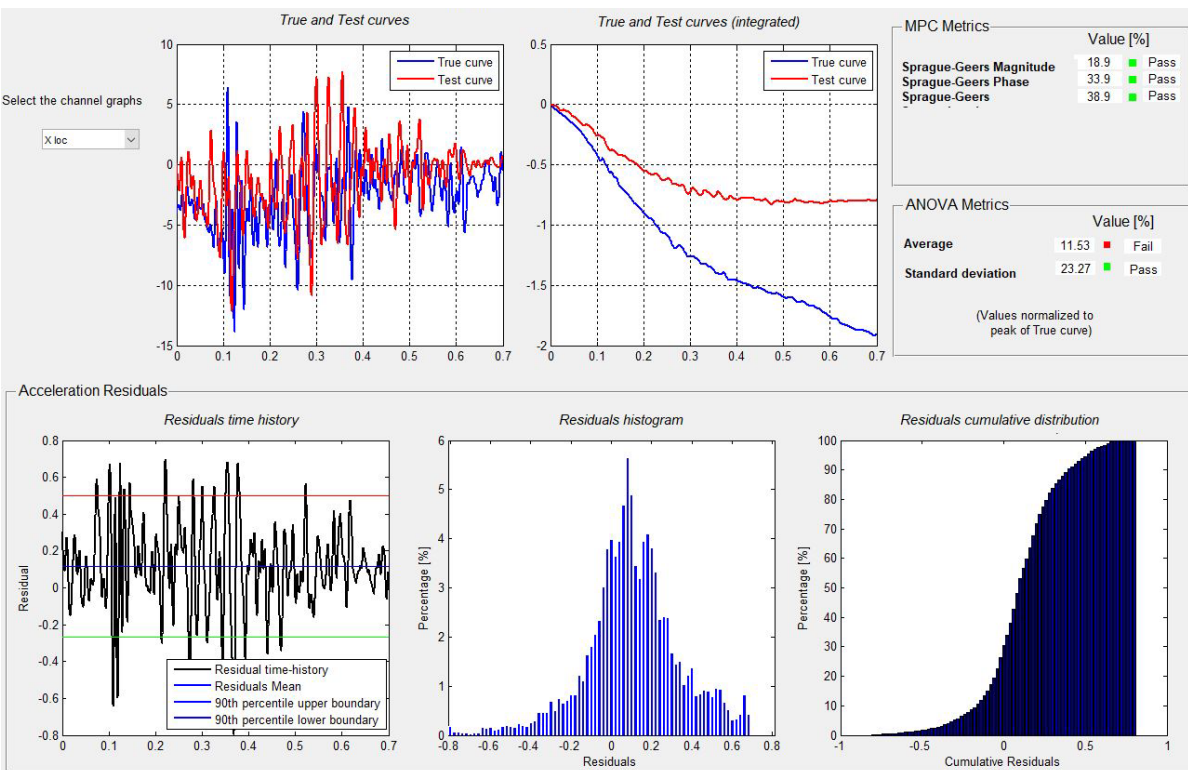


(b) 0.0 sec – 0.7 sec

Figure 3.5. RSVVP– Yaw Angle Validation Metrics.



(a) 0.0 sec – 0.3 sec



(b) 0.0 sec – 0.7 sec

Figure 3.6. RSVVP– X Acceleration (Longitudinal) Validation Metrics.

3.3. RETAINING WALL LOAD DISTRIBUTION

To determine the loading on a retaining wall installed adjacent to a W-beam guardrail system, the research team modified the validated model of the guardrail system by adding a rigidized retaining wall adjacent to the guardrail. This rigidized wall was setup to record lateral load distribution along the height of the wall due to the vehicle impact on the adjacent guardrail. The researchers varied the offset of the rigidized retaining wall from the guardrail and performed vehicle impact simulations for each offset to determine the load distribution on the retaining wall as a function of the lateral offset from the guardrail. Details of the modeling, simulation results, and the recommended load distribution for use in retaining wall design are presented in this section.

3.3.1. Model Setup

The soil around the guardrail posts was modeled as soil buckets that were 48 inches long (parallel to the W-beam rail) and 45 inches deep (below grade) (see Figure 3.1 and Figure 3.7) The nodes on the outer surfaces of the soil bucket, except the top surface and the surface against the rigidized retaining wall, were constrained.

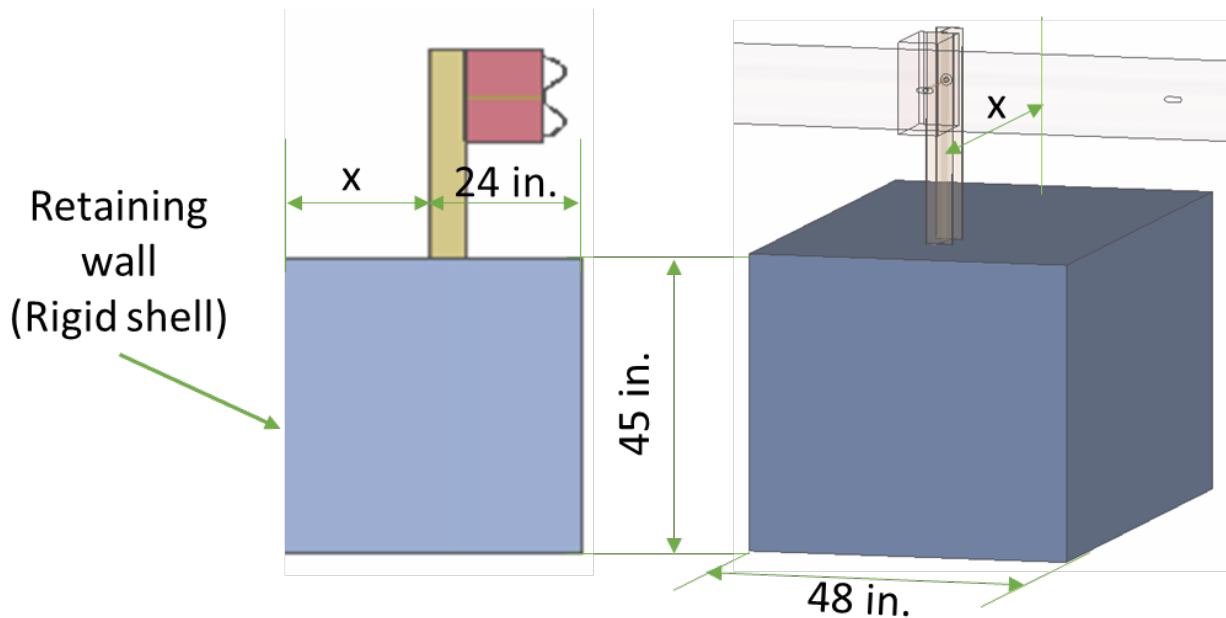


Figure 3.7. Soil Bucket Model and Dimensions.

The width of the buckets (perpendicular to the W-beam rail) was varied to allow different offsets of the W-beam guardrail from a rigidized retaining wall. The distance from the back of the post to the impact side of the soil bucket was fixed at 24 inches while the offset distance (x in Figure 3.7) was varied from 7 inches to 5 ft. The offsets modeled were 7 inches, 1 ft, 1.5 ft, 2 ft, 2.5 ft, 3 ft, 4 ft, and 5 ft.

For the W-beam guardrail post to function properly, it needs to deflect laterally and rotate when impacted by a vehicle. Restricting this lateral movement of the guardrail can lead to premature bending of the post, which can result in improper functioning of the guardrail. In previous MASH testing, the standard steel-post W-beam guardrail has successfully contained and redirected impacting vehicle when the posts were installed in concrete mow-strip with a 7-inch offset between the back of the post and the concrete cutout [9]. This testing shows that the 7-inch offset is sufficient to allow proper lateral deflection and rotation of the guardrail posts. For this reason, the research team selected 7 inches as the minimum offset for placement of the W-beam guardrail adjacent to a retaining wall. The maximum offset of 5 ft was selected after it was found that the retaining wall loading does not change significantly between the 4 ft and 5 ft offsets.

At each guardrail post location in the impact region, an idealized retaining wall with rigid material was modeled at the edge of the soil bucket. This wall was constrained in all directions and was setup to record contact loads due to the interaction with the adjacent soil and guardrail post during the vehicle impact simulation (Figure 3.8). To obtain a load distribution along the height of the retaining wall, the rigidized wall was setup to record loads in seven vertical load-recording regions, the heights of which varied with depth, as shown in Figure 3.8. The height of each load-recording region was varied to allow greater resolution near the top of the wall where the largest loads were expected. Figure 3.8 shows the depth of the center of each vertical load-recording region from grade.

Since a vehicle impacting a guardrail reaches each post at different times during the impact and redirection event, not all posts are loaded simultaneously. Similarly, depending on the speed and angle of the vehicle at each post, not all posts are loaded the same way. The researchers performed initial simulations and determined that the largest soil to wall lateral reaction forces occurred at the second post downstream of the impact point. This post location is shown in Figure 3.9. The retaining wall stress distribution profiles were developed using the forces at this post location. Stress at each load-recording region on the retaining wall was determined by dividing the total lateral reaction force measured for each region by its cross-sectional area.

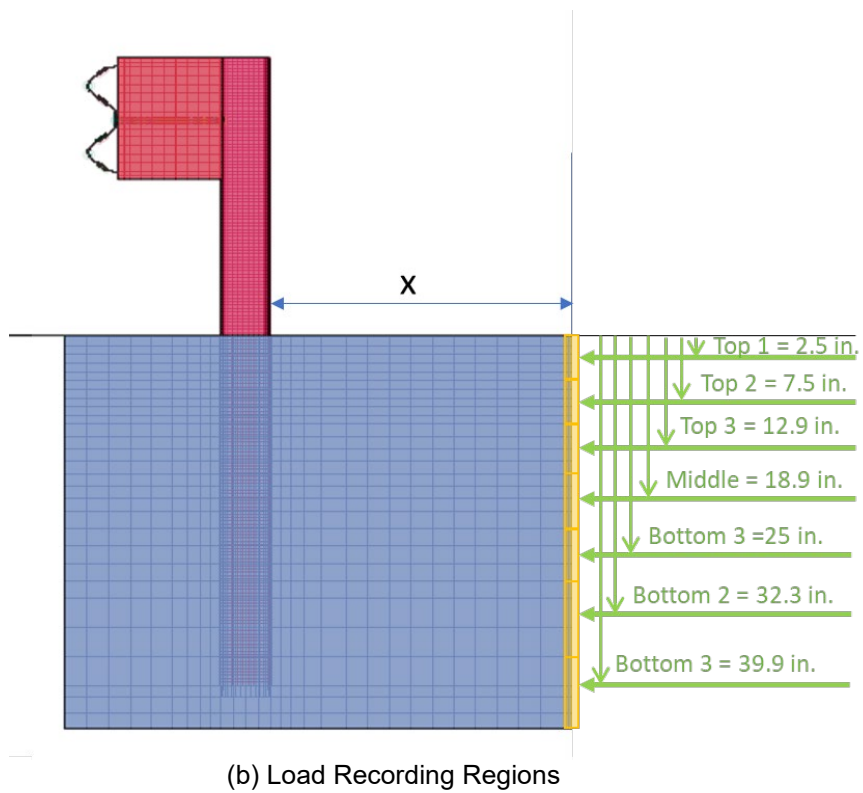
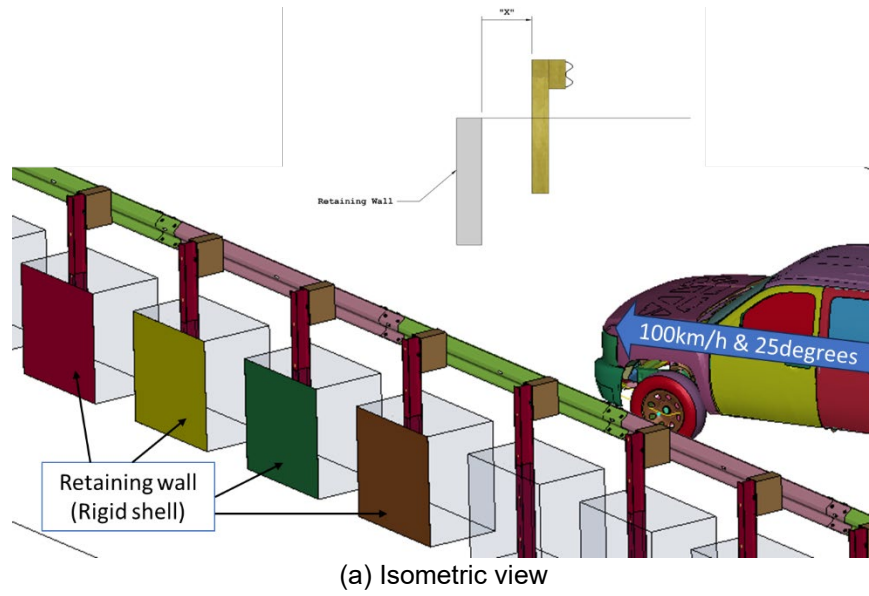


Figure 3.8. Isometric View of the System Model and Locations of Load-Recording Regions on the Retaining Wall.

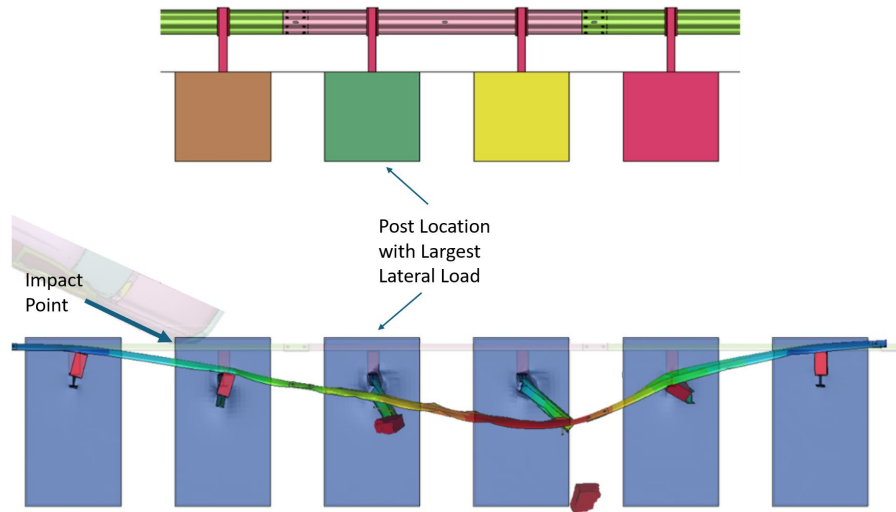


Figure 3.9. Location of Impact Point and Post with Largest Lateral Load.

3.3.2. Simulation Results

The research team performed vehicle impact simulations with W-beam guardrail system installed at various lateral offsets from the rigidized retaining wall. All simulations were performed using the impact conditions of MASH Test 3-11 with a 5,000-lb pickup truck impacting the guardrail at an impact speed and angle of 62 mi/h and 25 degrees, respectively. MASH Test Level 3 (TL-3) also specifies evaluating longitudinal barriers such as the W-beam guardrail with Test 3-10 using a 2,420-lb small passenger car. The small car impact is not expected to impart greater loading on the guardrail and the retaining wall compared to the heavier pickup truck. For this reason, simulations were only performed with the pickup truck using the Test 3-11 impact conditions.

As previously mentioned, eight different offsets of the retaining wall, ranging from 7 inches to 5 ft, were modeled and simulated. The impact conditions were the same for all simulations. Figure 3.10 and Figure 3.11 show sequential images of the impact simulations. The vehicle was successfully contained and redirected in all simulations and the W-beam guardrail functioned properly.

Offset	0.00 sec	0.33 sec	0.7 sec
7in			
1ft			
1.5ft			
2ft			

Figure 3.10. Sequential Images During Impact Simulations.

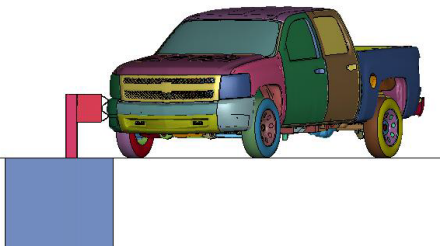
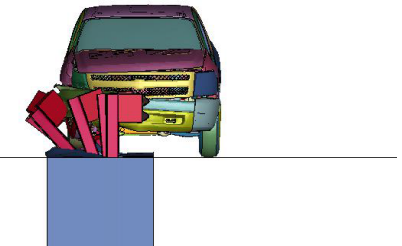
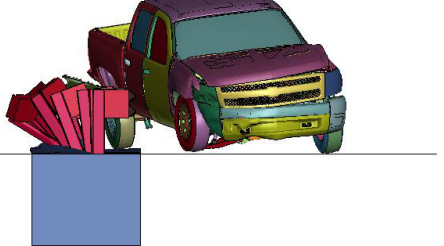
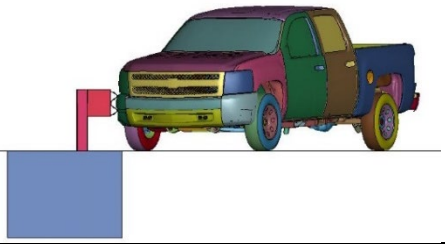
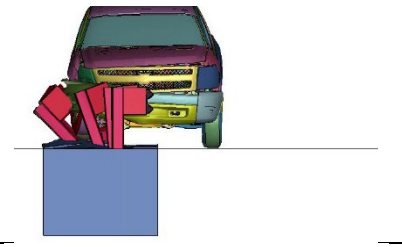
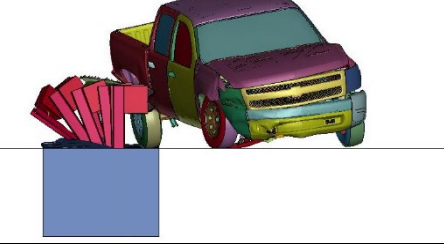
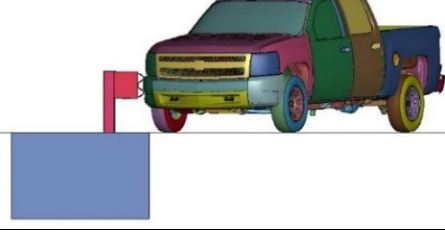
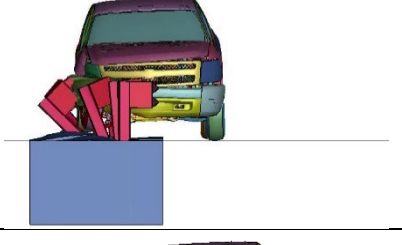
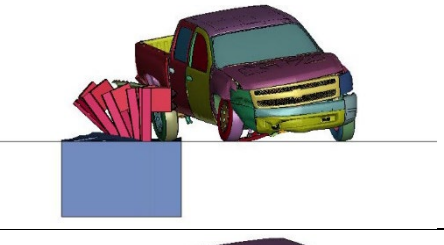
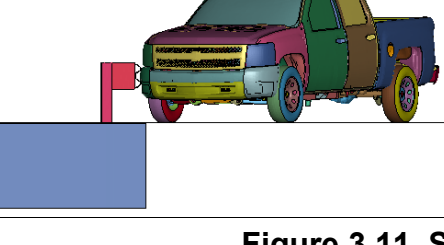
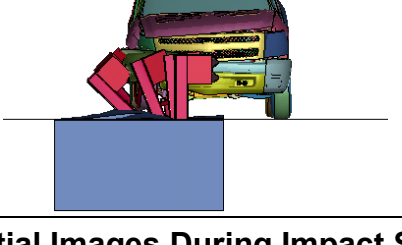
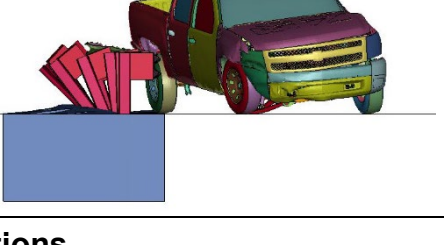
Offset	0.00 sec	0.33 sec	0.7 sec
2.5ft			
3ft			
4ft			
5ft			

Figure 3.11. Sequential Images During Impact Simulations.

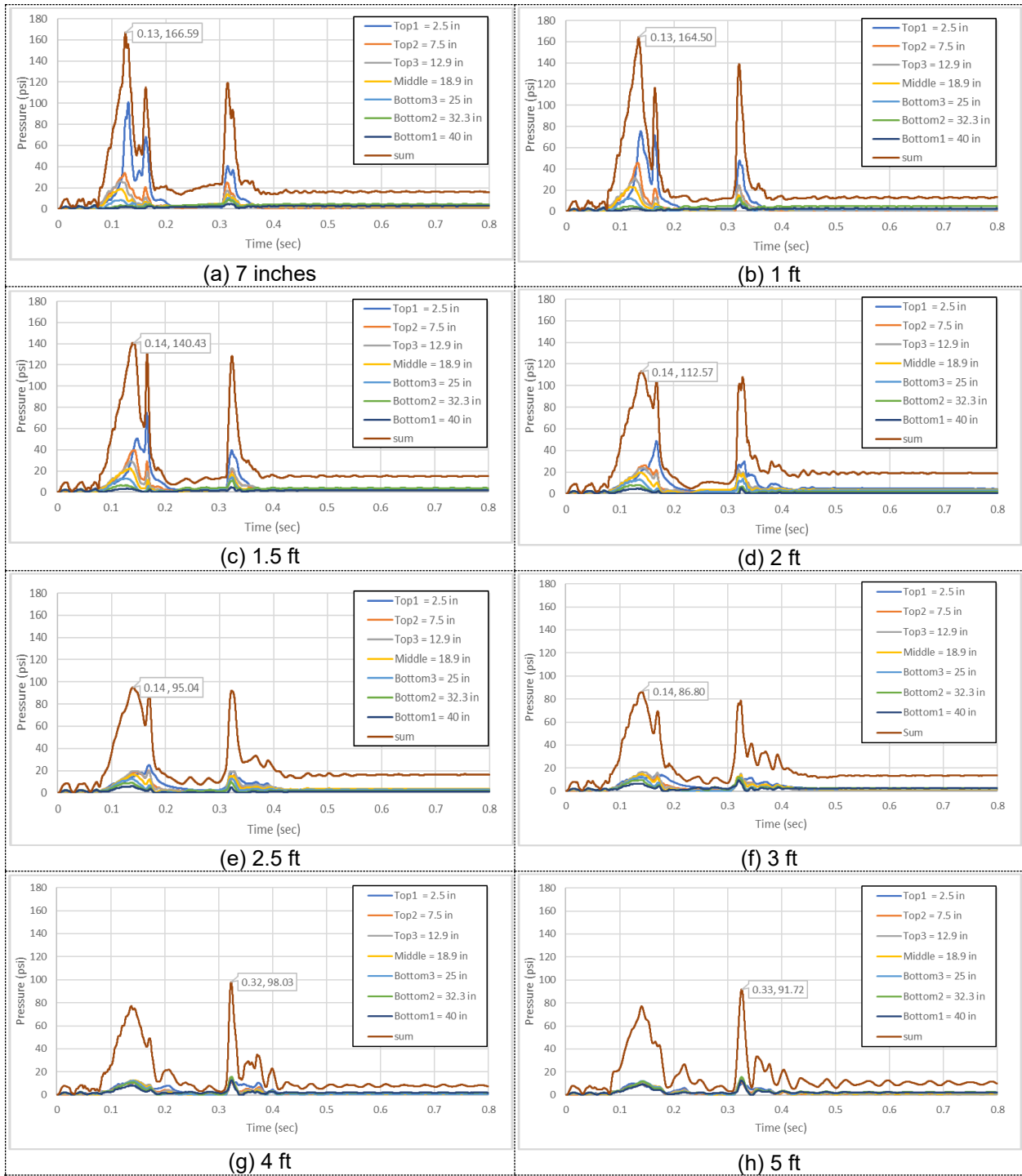


Figure 3.12. Pressure Loads on Retaining Wall for Different Offsets of the W-beam Guardrail.

Plots in Figure 3.12 show the pressure loading on the seven load-recording regions of the retaining wall, as well as the sum of all the loads for each retaining offset simulated. As previously shown in Figure 3.8, below-grade depth of the center of these load-recording regions ranged from 2.5 inches at the top to 40 inches at the bottom, denoted by “Top1” and “Bottom1” in Figure 3.12, respectively. The sum of pressure loading from all the load-recording regions is denoted as “sum” in each of the plots Figure 3.12.

In the impact simulations, two distinct peaks were observed in the pressure loading. The first peak occurred close to the time when the vehicle starts to redirect (between 0.13 – 0.14 seconds), and the second peak occurred near the time of the impact of the rear part of the vehicle into the guardrail, commonly referred to backslap from the vehicle (around 0.3 seconds). For each retaining wall offset, the researchers used the pressures from the load-recording regions at the time when the total pressure load for that offset was maximized. For retaining walls with offset distances less than or equal to 3 ft, the maximum loading occurred at the time of the first peak (i.e. start of vehicle redirection). For the 4 ft and 5 ft offsets, the maximum loading occurred at the time of the second peak (i.e. due to vehicle backslap).

Figure 3.13 shows the pressure distribution profile along the depth of the retaining wall, calculated over the load-recording regions when the overall pressure reaches the maximum value. The retaining wall offset in this case is 3 ft. Similar pressure distributions were developed for all offsets and were combined to develop the pressure versus depth plot shown in Figure 3.14. The curves in the plot represent different retaining wall offsets used in the simulation analyses.

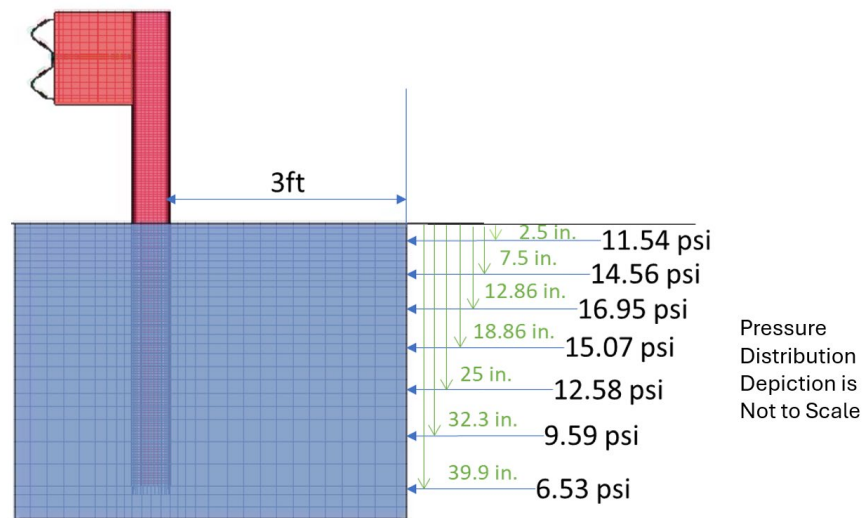


Figure 3.13. Pressure Distribution on Retaining Wall with 3-ft Offset.

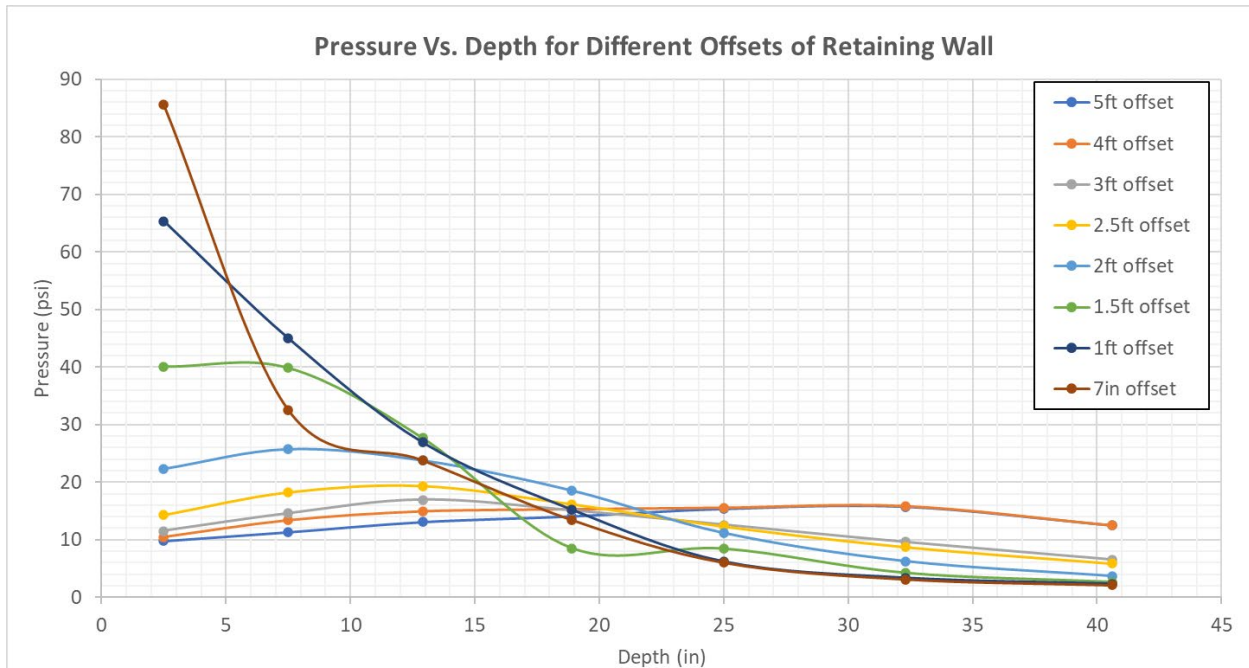


Figure 3.14. Pressure on Retaining Wall as a Function of Depth.

For posts installed very close to the retaining wall (7-inch to 1.5-ft offset), the loading from the vehicle impact is the highest near the top of the adjacent retaining wall. This is expected since maximum lateral deflection of the guardrail post occurs near the top, which applies the greatest load on the retaining wall. As the lateral offset is increased, pressure on the retaining wall gradually increases with depth before dropping off.

Figure 3.15 demonstrates the use of the plots presented in Figure 3.14. A W-beam guardrail system is shown installed adjacent to a retaining wall at an offset x from the wall. The posts of the standard W-beam guardrail are embedded 42 inches into the soil. The example in Figure 3.15 shows loading on the retaining wall for a W-beam guardrail system installed with a 7-inch offset from the wall. Using the curve representing the 7-inch offset in Figure 3.14, pressure distribution on the wall was determined at various depths at a 2.5-inch increment. The corresponding pressure distribution along the depth of the guardrail post is shown in Figure 3.15. This loading should be incorporated in the retaining wall design calculations to accommodate additional loading that may be applied to the retaining wall in the event of a vehicle impact on the guardrail installed with the 7-inch offset from the wall.

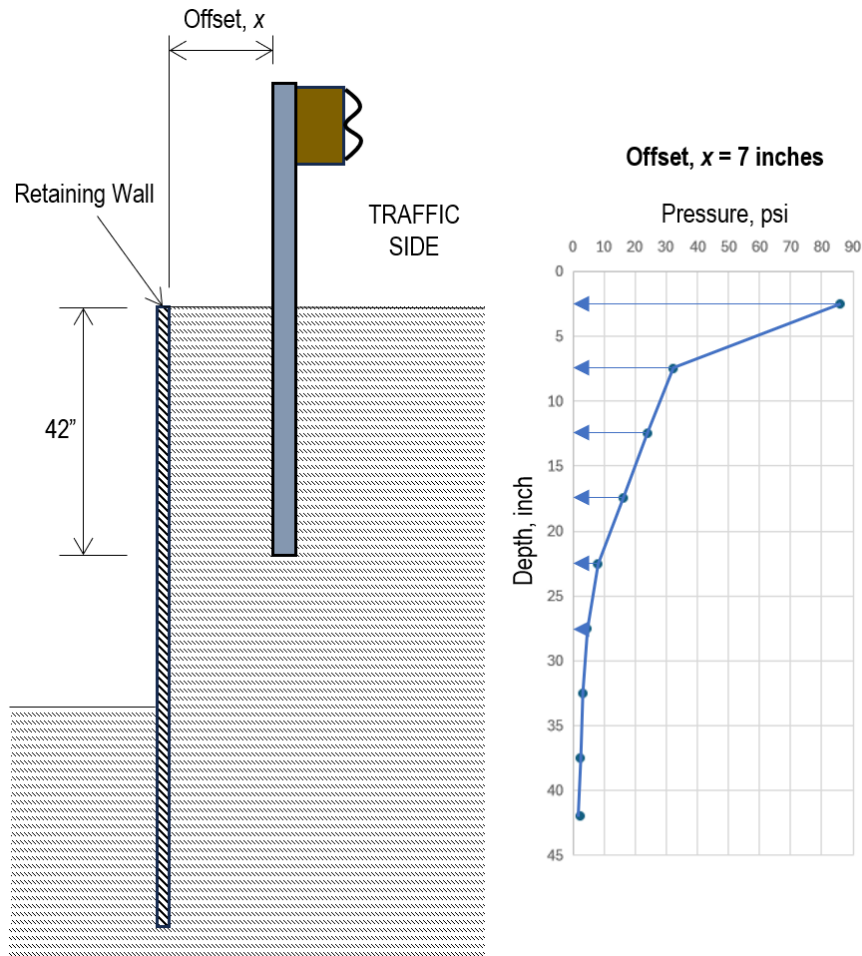


Figure 3.15. Pressure Loading on a Retaining Wall due to Impact on a W-beam Guardrail at 7-inch Offset.

3.3.3. Implementation

The pressure distribution presented in Figure 3.14 can be used by engineers and designers to determine the additional loading on a retaining wall due to a potential vehicle impact on a W-beam guardrail installed near the wall. It is recommended that this pressure loading be incorporated into the retaining wall design process to accurately account for the vehicle impact load on an adjacent W-beam guardrail.

The retaining wall in this research was modeled as an idealized rigid wall. While there are many types of retaining walls, (concrete, sheet pile, etc.), and they vary in strength and load bearing capacity, the pressure loading developed in this research with the rigidized retaining wall can be used for all types of retaining walls.

Chapter 4. SUMMARY AND CONCLUSIONS

This research determined the minimum lateral offset needed for installing the standard W-beam guardrail system adjacent to rip rap, such that there is minimal damage to the rip rap if a vehicle strikes the guardrail. The research team used results of a past crash test with the W-beam guardrail system to determine the lateral offset needed to achieve minimal disturbance of rip rap and to ensure proper functioning of the guardrail. This distance was determined to be 44 inches from the back of the guardrail posts. It should be noted that extra offset may be required for guardrail end terminals due to additional impact performance requirements. Manufacturer's guidance should be followed for determining the appropriate offset for guardrail end terminals.

The researchers also determined the pressure loading on a retaining wall that is installed near a W-beam guardrail and is hit by an errant vehicle. The researchers performed vehicle impact simulations of the W-beam guardrail system installed adjacent to a retaining wall with various offsets. Using the results of these simulations, the researchers developed a pressure distribution for incorporating into the retaining wall design process to account for the potential of a vehicle impact on an adjacent W-beam guardrail system. This pressure loading is shown in Figure 3.14 and is a function of the depth of the retaining wall and the offset of the wall from the W-beam guardrail system. By integrating this pressure loading into the retaining wall design process, engineers can accurately account for vehicle impact loads on an adjacent W-beam guardrail.

For the W-beam guardrail to function properly, the guardrail should have a minimum 7-inch offset from the retaining wall. Installing the guardrail closer than 7 inches of a retaining wall is likely to restrict the movement of the guardrail posts on vehicle impact, which can lead to guardrail malfunction. If site conditions do not allow having the minimum 7-inch offset from the retaining wall, a different barrier type should be considered instead of the W-beam guardrail (e.g., a concrete or metal bridge rail).

The scope of this research focused on the standard W-beam guardrail system which is a MASH TL-3 system that has been designed to contain and redirect a 5,000-lb vehicle impacting the guardrail at an impact speed and angle of 62 mph and 25 degrees, respectively. Results of this research are therefore primarily applicable for this specific guardrail system. If a higher Test Level guardrail is installed next to a retaining wall, such as a Test Level 4 (TL-4) guardrail that is designed to contain and redirect a 22,000-lb single unit truck impacting at a speed and angle of 56 mph and 15 degrees, higher loads will be applied to the wall that were not evaluated in this research. Furthermore, there are other TL-3 guardrail systems that may have higher loading capacity than the standard W-beam guardrail (e.g., three beam guardrail, reduced post spacing W-beam guardrail, etc.). These systems may also impart higher load on the wall than the standard W-beam guardrail design evaluated in this research.

The pressure loading guidance developed in this research may also be used for a W-beam guardrail end terminal that is installed close to a retaining wall. However, the Roadside Design Guide (RDG) and the guardrail end terminal manufacturer's guidelines should be followed to allow sufficient offset between the end terminal and any adjacent vertical drop that may destabilize a vehicle impacting in the end terminal region.

REFERENCES

1. Sweigard, M.E., K.A. Lechtenberg, R.K. Faller, J.D. Reid, and E.L. Urbank. *MASH 2016 Test No. 3-10 of MGS Installed in an Asphalt Mow Strip with Nearby Curb (Test No. GAA-1)*. Midwest Roadside Safety Facility, Report TRP-03-377-17, Lincoln, Nebraska, 2017.
2. AASHTO. *Manual for Assessing Safety Hardware*, Second Edition. American Association of State Highway and Transportation Officials, Washington, DC, 2016.
3. Polivka, K. A., Faller, R. K., Sicking, D. L., Rohde, J. R., Bielenberg, B. W., & Reid, J. D. (2006). *Performance Evaluation of the Midwest Guardrail System – Update to NCHRP 350 Test No. 3-11 with 28" C.G. Height (2214MG-2)*. Report No. TRP-03-171-06. Midwest Roadside Safety Facility (MwRSF). University of Nebraska-Lincoln, Lincoln, NE.
4. Livermore Software Technology Corporation. (2019). *LS-DYNA keyword user's manual (Version R10.1)*. Livermore, CA: LSTC.
5. National Crash Analysis Center. (2007). *2007 Chevrolet Silverado Finite Element Model (Version 1.0)*. The George Washington University, Ashburn, VA.
6. Bligh, R. P., Ross, H. E. Jr., Epperson, B., and Sherry, K. (2000). *Test Risk Assessment Program (TRAP): Version 2.1*. Report No. FHWA-RD-99-162. Texas A&M Transportation Institute (TTI), Texas A&M University Systems, College Station, TX.
7. National Crash Analysis Center. (2010). *Roadside Safety Verification and Validation Program (RSVVP) Manual (Version 3.0)*. The George Washington University, Ashburn, VA.
8. Ray, M. H., Mongiardini, M., Plaxico, C. A., & Anghileri, M. (2010). *Procedures for Verification and Validation of Computer Simulations Used for Roadside Safety Applications*. National Cooperative Highway Research Program, NCHRP Project 22-24 Report, NCHRP Web-Only Document 179.
9. Sheikh, N.M., Menges, W.L., and Kuhn, D.L. (2019). *MASH TL-3 Evaluation of 31-inch W-Beam Guardrail with Wood and Steel Posts in Concrete Mow Strip*. Test Report No. 608551-1-4. Texas A&M Transportation Institute (TTI), Texas A&M University Systems, College Station, TX.

APPENDIX A

Following is a list of research that has been performed to address movement of the posts in soil for successful W-beam guardrail performance.

- FHWA. FHWA Memorandum Technical Summary Force-Deflection Characteristics of Guardrail Posts. FHWA; 1988.
- Herr JE, Rohde JR, Sicking D, Reid J, Faller RK, Holloway J, et al. Development of Standards for Placement of Steel Guardrail Posts in Rock. MwRSF; 2003.
- Bligh RP, Seckinger RN, Abu-Odeh AY, Roschke PN, Menges WL, Haug RR. Dynamic Response of Guardrail Systems Encased in Pavement Mow Strips. TTI; 2004. Report No.: FHWA/TX-04/0-4162-2.
- Sheikh NM. TTI Technical Memorandum Guidelines for W-Beam Guardrail Post Installation in Rock. TTI; 2009. Report No.: 405160-7—1.
- Arrington D, Bligh RP, Menges WL. Alternative Design of Guardrail Post in Asphalt or Concrete Mowing Pads. TTI; 2009.
- FHWA. FHWA Memorandum Application and Installation of Roadside Hardware Revised Nov. 3, 2010. 2010.
- New Zealand Transport Agency. Technical Memorandum TM-2005 Using Low Strength Concrete Around Guardrail Posts. 2011.
- Whitesel D, Jewell J, Meline R. Development of Weed Control Barrier Beneath Metal Beam Guardrail. CALTRANS; 2011. Report No.: FHWA/CA10-0515.
- Lee SH, Bakhtiary E, Stewart LK, Scott D, White D. Effect of Pre-Cut Asphalt Fracture Planes On Highway Guardrail Performance. International Journal of Computational Methods and Experimental Measurements. 2016;4(3):353-63.
- FHWA. Web Page FHWA Q and A on Barriers Accessed 2017
- Sweigard M, Lechtenberg K, Faller R, Reid J, Urbank E. MASH 2016 Test No. 3-10 of MGS Installed in an Asphalt Mow Strip with Nearby Curb (Test No. GAA-1). MwRSF; 2017. Report No.: TRP-03-377-17.
- Lee S-H, Bakhtiary E, Scott D, Stewart L, White D. Influence Of Geometric Parameters On The Restraint Of Guardrail Posts By Asphalt Mow Strips. Sustainable and Resilient Infrastructure. 2017.
- Scott DW, Stewart LK, White DW, Bakhtiary E, Lee SH. Dynamic Subcomponent Testing and Finite Element Simulation of Guardrail Systems with Alternative Post Installation Methodologies. Georgia; 2018. Report No.: FHWA-GA-18-1508.
- Bligh RP, Menges WL, Griffith B, Schroeder G, Kuhn DL. MASH Evaluation of TxDOT Roadside Safety Features - Phase II. TTI; 2019. Report No.: FHWA/TX-18/0-6946-R2.

- Sheikh NM, Menges WL, Kuhn DL. MASH TL-3 Evaluation of 31-Inch W-beam Guardrail with Wood and Steel Posts in Concrete Mow Strip. TTI; 2019. Report No.: 608551-1-4.
- Moran S, Bligh R, Menges WL, Schroeder G, Kuhn DL. MASH Test 3-11 Evaluation Of TxDOT W-Beam Guardrail With 7½-Inch Diameter Round Wood Posts In Concrete Mow Strip. TTI; 2020. Report No.: FHWA/TX-19/0-6968-R2.
- Sheikh NM, Bligh R, Bastin B. Design and Evaluation of Asphalt Vegetation Control Treatment for Steel-Post W-Beam Guardrail System. TTI; 2024. Report No.: 619441-01-0910.